HYDRODYNAMIC ANALYSIS OF A FIXED INCLINE SLIDER BEARING

BY

LIMO K. JOSHUA

A THESIS SUBMITTED IN PARTIAL FULFILLMENT OF THE REQUIREMENT FOR AWARD OF A DEGREE OF DOCTOR OF PHILOSOPHY IN APPLIED MATHEMATICS OF UNIVERSITY OF ELDORET, KENYA

FEBRUARY, 2016

DECLARATION

This thesis is my original work and has not been presented for the award of a degree in any other University. No part of this thesis may be reproduced without the prior written permission of the author /or University of Eldoret.

Limo Joshua Kipkorir

Signature.....

Date.....

SC/PHD/M/19/2012

This thesis has been submitted for examination with our approval as University Supervisors.

1. **Prof. Jacob K. Bitok**
   Department of Mathematics
   and Computer Science
   University of Eldoret

   Signature..... Date.....

2. **Prof. Alfred W. Manyonge**
   Department of Pure and
   Applied mathematics
   Maseno University

   Signature..... Date.....

DEDICATION

To my primary school teacher Mr. Job Kipng'eny who made me to develop interest in mathematics, my high school teacher Mr. John Mwangi, my college tutor Mr. Agunda Lwande who taught me calculus and analytical geometry, my university lecturer Prof. Matthew Kinyanjui who introduced me to Ordinary Differential Equations and Fluid Dynamics, my beloved wife Stella and my three daughters, Angela, Kate and Valerie, who were very understanding when I was busy studying, you will forever remain special to me.

ABSTRACT

In the present day technological scenario, machines rotating at high speeds and carrying heavy rotor loads are used. As a result, fixed incline slider bearings are used. They are designed for high axial loads. When a bearing rotates at high speed, the heat generated due to large shearing rates in the lubricant film raises its temperature which lowers the viscosity of the lubricant and in turn affects the performance characteristics of the bearing. Hydrodynamic analysis should therefore be done to obtain the realistic performance characteristics of the bearing. In most of the analyses, two dimensional energy equation is used to find the temperature distribution in the fluid film by neglecting the temperature variation in the axial direction. In this research, two dimensional study was done to predict pressure distribution along a fixed incline slider bearing surface axially and across the film thickness. Two dimensional energy equation was also used to obtain the temperature distribution in the fluid film by considering the temperature distribution in the axial direction. It was found that the Pressure distribution increases with decreasing film thickness ratio i.e. as the film thickness ratio becomes smaller, the pressure profile increases without limits and that the normal load carrying capacity, the adiabatic temperature of a fixed incline slider bearing increases with decreasing film thickness ratio. Also, it was established that the film thickness ratio increases as the friction coefficient increases and that there will be a greater power loss in a fixed incline slider bearing when the film thickness ratio is small. The results obtained here will be useful in designing and modifying fluid dynamic bearings.

TABLE OF CONTENTS

LIST OF TABLES

LIST OF FIGURES

LIST OF ABBREVIATIONS

Symbol	Meaning	Units
A, B,C and D	Integration constants	
X, Y and Z	Dimensionless length parameters	
h	Oil Film thickness	m
h_m	Maximum Film thickness	
h_0	Characteristic length in the z direction	m
l_0	Characteristic length in x direction	m
p	Pressure	Pa
P	Dimensionless pressure,	
p_0	Characteristic pressure	Pa
q	Fluid velocity vector	ms^{-1}
u, v, w	Velocity components in the x, y and z directions respectively	ms^{-1}
u_0	Characteristic velocity in the x direction	ms^{-1}
v_0	Characteristic velocity in the y direction	ms^{-1}
z_0	Characteristic velocity in the z direction	ms^{-1}
t	Time	s
T	Dimensionless time	
τ	Viscous shear stress	N/m^2
ρ	Fluid density,	Kgm^{-3}
ρ_m	Maximum density	Kgm^{-3}
η	Absolute viscosity	Pas
η_0	Characteristic Absolute viscosity,	Pas

T_0	Characteristic temperature	K
C_p	Specific Heat	$Jkg^{-1}k^{-1}$
K	Thermal conductivity	$Wm^{-1}k^{-1}$
P_r	Prandlt number	
P_c	Pressure coefficient	
R_e	Reynolds number	
S_t	Stribeck number	
H_0	Oil film thickness in the leading edge	m
$\vec{\nabla}$	Gradient operator $\left(= \mathbf{i}\frac{\partial}{\partial x} + \mathbf{j}\frac{\partial}{\partial y} + \mathbf{k}\frac{\partial}{\partial z} \right)$	
∇^2	Laplacian operator $\left(= \frac{\partial^2}{\partial x^2} + \frac{\partial^2}{\partial y^2} + \frac{\partial^2}{\partial z^2} \right)$	
N	Relative speed,	
p_{av}	Average bearing pressure.	

ACKNOWLEDGEMENT

I take this opportunity to thank the almighty God for the gift of life and for enabling me to undertake this research. This work would never have been possible without close and strict supervision and guidance from Prof. Jacob K. Bitok of University of Eldoret and Prof. Alfred W. Manyonge of Maseno University. I am thankful for their time and tireless efforts invested in me, for sharing their ideas, reading material and providing feedback when necessary. My special thanks to the Dean School of Science Dr. Victor Kimeli and Chairman of the Department of Mathematics and Computer science, Dr. Betty Korir for their encouragement. I also will not forget to thank Dr. P.R. Kiogora (Jkuat), Dr. Argwings Otieno, Dr. Julius Shichikha and Mrs. Lillian Kangogo from University of Eldoret for their inspiration and support. I also wish to pass my sincere gratitude to my classmates; Bundotich, Mumo, Saina and Kandie for encouraging me to undertake this research.

CHAPTER ONE

INTRODUCTION

1.1 Background Information

Machines consist of elements and their safe and efficient operation relies on carefully designed interfaces between these elements. The functional design of interfaces cover geometry; materials, lubrication and surface topography, and an incorrect design may lead to both lowered efficiency and shortened service life. A misalignment due to geometrical design could lead to large stress concentrations that in turn may lead to severe damage when mounting, a detrimental wear situation and rapid fatigue during operation. Large stress concentrations also implicitly imply a temperature rise because of the energy dissipation due to plastic deformations. This means that the choice of mating materials is also of great importance such as, electrolytic corrosion may drastically reduce service life. Contact fatigue due to low ductility would not only lower the service life but could lead to third body abrasion due to sparling, which in turn could end up lowering the service life of other components. A lubricant serves several crucial objectives; with its main objective being to lower friction, the actions of additives are of concern. If the interface is subjected to excessive wear, the lubricants ability to form a separating film becomes even more crucial. In this case, the bulk properties of the lubricant have to be carefully chosen. At some scale, regardless of the surface finish, all real surfaces are rough and their topography influences the contact condition. As implied above, these design parameters are mutually dependent i.e. they affect the way lubricants properties and geometry influence the operation of the system. For example, a change in geometry could require another choice of materials that may change the objectives of the lubricant and force the operation into another lubrication regime. All the four design parameters are

of great importance. However, in this research, focus will be on the lubricant properties such as pressure, temperature, viscosity and the geometry of the bearing and how it affects the performance characteristics of the bearing.

1.2 Basic Concepts

Whenever two bodies in contact are made to slide relative to one another, a resistance to the motion is experienced. This resistance, called friction is present in all machinery. Approximately 30% of the power of an automobile engine is consumed by friction. Friction and wear can be significantly reduced and this relative motion of machine parts made possible, by interposing a substance at the interval of the contacting surfaces. Lubrication refers to the reduction of friction by interposing suitable material between the two surfaces in contact and in relative motion. The substance between the two surfaces is known as a lubricant. The interposed lubricant film can be a solid, solid/liquid dispersion, a liquid, liquid-liquid dispersion or gas. Mineral oils manufactured from petroleum are the most common liquid lubricants. The manufacturer of petroleum lubricants can choose from a wide variety of crude oils, and the choice is of great importance because the lubricating oil fraction of crude oil varies widely. The machine elements designed to carry out lubrication are called bearings**.** The science and technology of interacting surfaces in relative motion is called tribology.

1.2.1 Heat Transfer in lubricants

Friction in bearings causes an increase of the temperature inside the bearing. If the heat produced cannot be adequately removed from the bearing, the temperature might exceed a certain limit and as a result, the bearing would fail. Bearings are commonly used in mechanical systems when there are rotating parts in the systems. For bearings that run at high speeds above 1,000 revolutions per minute, such as those used in aircraft turbines, machining tools and automotive engines, it is important to take into account the heat transfer through bearing system due to friction. Heat transfer is generally not considered for applications where the bearing is rotating at low speeds such as clocks and bicycles. However, for certain aerospace applications, such as precision instruments or wind turbines, the heat transfer through the bearing becomes relevant.

1.2.2 Viscosity

Viscosity is a physical measurement of a fluids' internal resistance to flow. Assume that a lubricating film is compressed between two flat plates creating a film between the plates. Force is required to make the plates move or overcome the fluids film friction. This force is known as dynamic viscosity. Dynamic viscosity is a measurement of lubricants internal friction. A common tool used to measure dynamic viscosity is the Brookfield viscometer. A more familiar viscosity term is Kinematic viscosity which takes into account the fluids density as a quotient of the fluids dynamic viscosity. The Kinematic viscosity is determined by using a capillary

viscometer in which a fixed volume of a fluid is passed through a small orifice at a controlled temperature under the influence of gravity.

Various conditions must be considered when specifying the proper viscosity of a lubricant for a given application. These conditions include the operating temperature, the speed at which the specific part is moving and the load placed upon the part. One other consideration is whether or not the lubricant can be contained so that it remains present to lubricate the intended moving part.

1.2.3 Temperature

The viscosity of a lubricant changes with temperature. As temperature increases, the viscosity decreases. Conversely, as temperature decreases, the viscosity increases. To select a proper lubricant for a given application, the viscosity of a fluid must be high enough so as to provide adequate lubricating film, but not so high that friction within the lubricating film is excessive. Therefore when a piece of equipment must be started or operated at either temperature extreme, hot or cold, the proper viscosity must be considered.

1.2.4 Speed

The speed at which a piece of equipment operates must also be considered when specifying the proper lubricant viscosity. In high speed equipment, a high viscosity lubricant will not flow well in the contact zones and will channel out by fast moving elements of the equipment. On the other hand, low viscosity lubricant will have too

low viscosity to properly lubricate slow-moving equipment, because it would run right out of the contact zone.

1.2.5 Load

Equipment loads must also be considered when selecting the proper lubricant viscosity. Under a heavy load, the lubricant film is squeezed or compressed. Therefore a high viscosity lubricant is needed. The higher the viscosity, the more film strength the lubricant will generally possess. In addition, the load can be either a continuous or a shock load. A continuous load is a steady load that is maintained while the equipment is operational, while a shock load is a pounding or non-steady load. Under shock load conditions, a low viscosity lubricant would not possess enough film strengths to stay in place whereas a high viscosity lubricant could stay in place and act like a cushion in the contact area.

1.3 Regimes of Lubrication

When the load between the contact surfaces is progressively increased, three distinct situations may be observed with respect to the mode of lubrication, which are called regimes of lubrication namely;

1.3.1 Fluid Film Lubrication:

This is the lubrication regime in which through viscous forces, the load is fully supported by the lubricant within the space or gap between the parts in motion relative to one another (the lubricated conjunction) and solid-solid contact is avoided. There are two special cases of fluid film lubrication namely;

1.3.1.1 Hydrostatic lubrication:

This is a case of fluid-film lubrication in which an external pressure is applied to keep the lubricant in the conjunction, enabling it to support the external load. Figure 1.1 below illustrates hydrostatic lubrication.

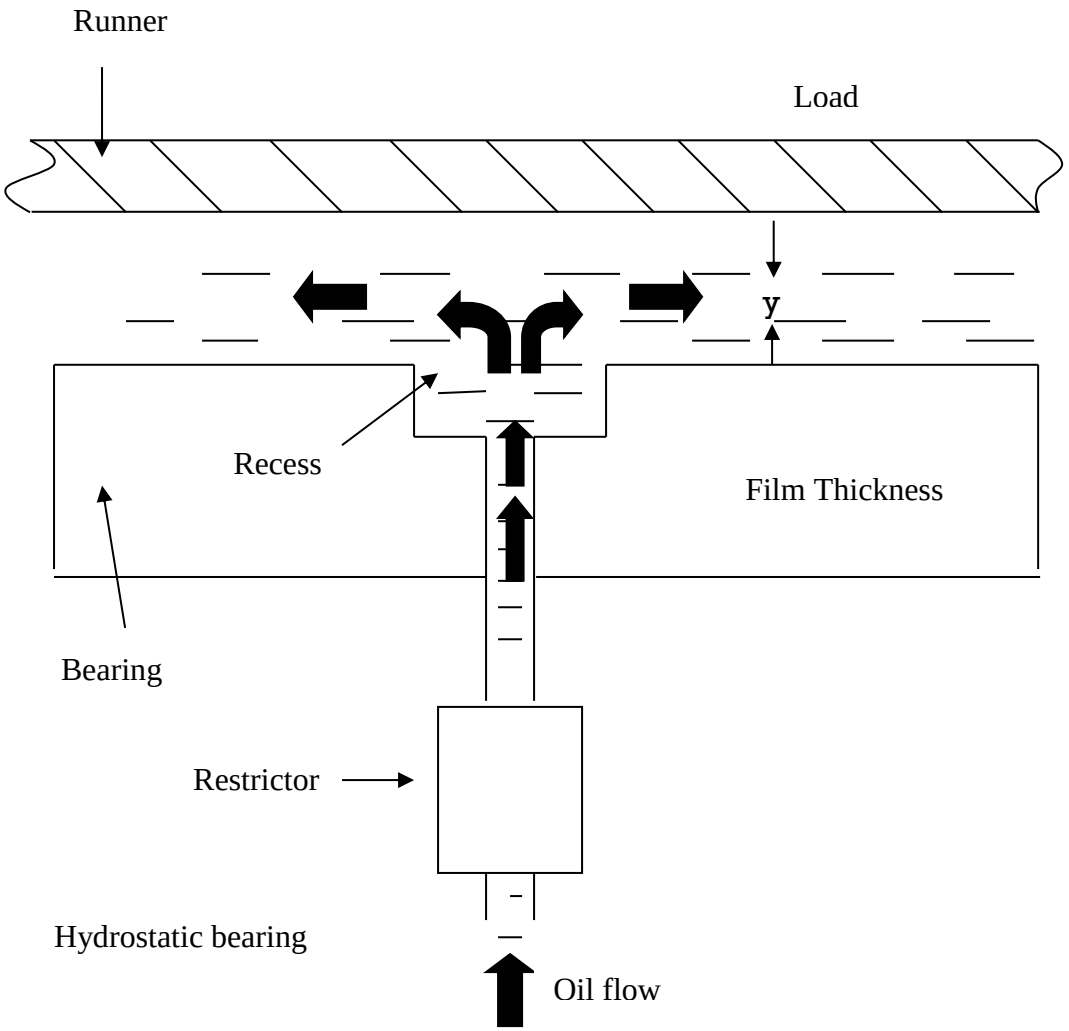

Figure 1.1: Hydrostatic Lubrication (Source; Author, 2015)

1.3.1.2 Hydrodynamic/Hydraulic lubrication**:**

This is a case of fluid-film lubrication which occurs when the lubricant is able to support the load without external pressure through hydrodynamic forces alone, which deform the shape of the interposing lubricant film into a wedge shape and drags the lubricant into the film so that the externally applied load can be supported. Figure 1.2 below illustrates hydrodynamic lubrication.

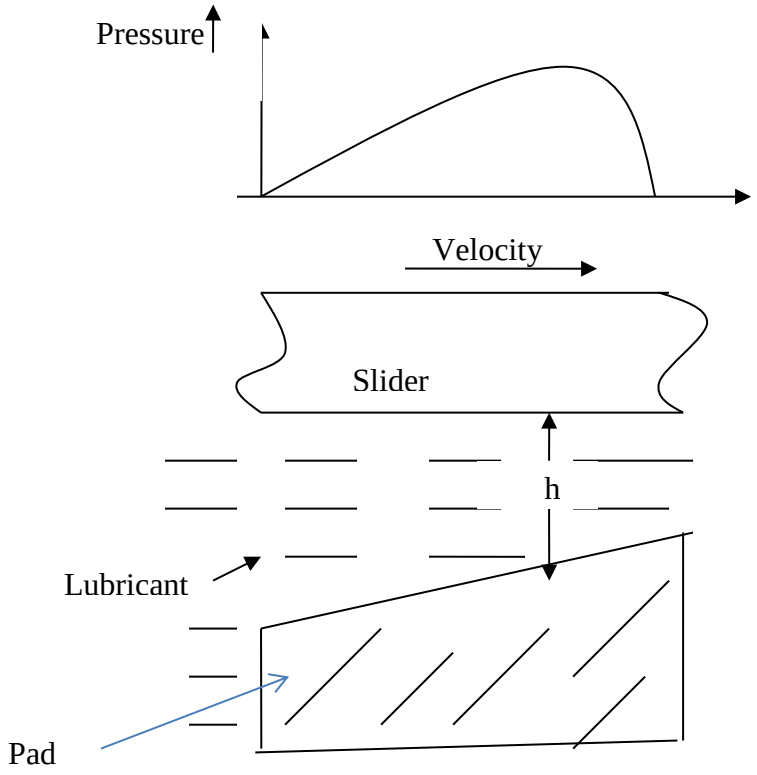

Figure 1.2: Hydrodynamic lubrication (Source; Author, 2015)

1.3.2 Elasto-hydrodynamic lubrication/mixed lubrication

The opposing surfaces are separated but there occurs some interaction between the raised solid features called asperities and there is an elastic deformation on the contacting surfaces enlarging the load bearing area where by the viscous resistance of the lubricant becomes capable of supporting the load.

1.3.3 Boundary lubrication

Here, the surfaces come into closer contact at their asperities (raised solid features). The heat developed by the local pressures causes a condition which is called stick-slip and some asperities break-off. At the elevated temperature and pressure conditions, chemically reactive constituents of the lubricant react with the contact surface forming a highly resistant tenatious layer, or film on the moving solid surfaces(boundary film) which is capable of supporting the load and major wear or breakdown is avoided. Boundary lubrication is also defined as that regime in which the load is carried by the surface asperities rather than by the lubricant. The lubrication regimes discussed above can be represented on a stribeck curve as shown in figure 1.3 below;

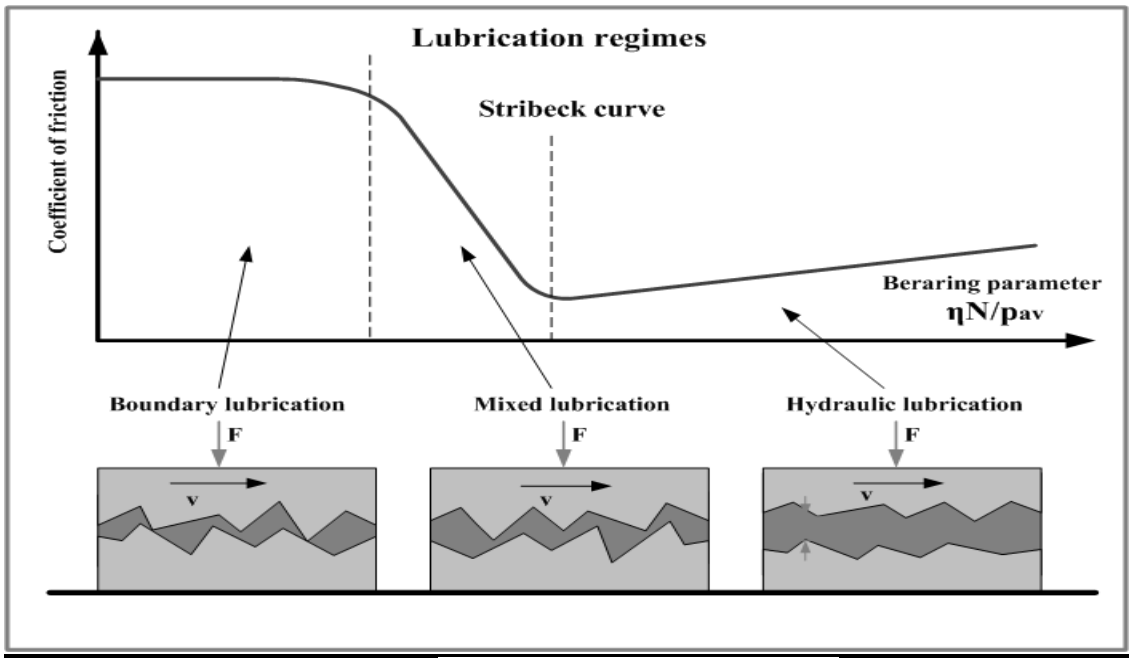

Bearing Parameter $\eta N/p_{av}$

Figure 1.3: Stribeck curve (Source; www.subtech.com, 2015)

The three lubrication regimes are clearly distinguished in the Stribeck curve in figure 1.3 above, which demonstrates the relationship between the coefficient of friction and

the bearing parameter $\eta N/p_{av}$. Stability of different lubrication regimes may be explained by means of the Stribeck curve. Temperature increase due to heat generated by friction causes drop of the lubricant viscosity and the bearing parameter. According to the Stribeck curve decrease of the bearing parameter in mixed regime causes increase of the coefficient of friction followed by further temperature rise and consequent increase of the coefficient of friction. Thus mixed lubrication is unstable. Increase of the bearing parameter due to temperature rise (lower viscosity) in hydrodynamic regime of lubrication causes the coefficient of friction to drop with consequent decrease of the temperature. The system corrects itself. Thus hydrodynamic lubrication is stable

1.4 Types of bearings

Bearings are machine elements designed to carry out lubrication. There are various types of bearings. A thrust bearing is a particular type of rotary rolling-element bearing. Like other bearings they permit rotation between parts, but they are designed to support a predominately axial load. Thrust bearings come in several varieties namely; Thrust ball bearings, cylindrical thrust roller bearings, tapered roller thrust bearings, spherical roller thrust bearings, fluid bearings and magnetic bearings. Thrust ball bearings, composed of ball bearings supported in a ring, can be used in low thrust applications where there is little axial load. Cylindrical thrust roller bearings consist of small cylindrical rollers arranged flat with their axes pointing to the axis of the bearing. They give very good carrying capacity and are cheap, but tend to wear due to the differences in radial speed and friction which is higher than with ball bearings. Tapered roller thrust bearings consist of small tapered rollers arranged so that their axes all converge at a point on the axis of the bearing. The length of the roller and the

diameter of the wide and the narrow ends and the angle of rollers need to be carefully calculated to provide the correct taper so that each end of the roller rolls smoothly on the bearing face without skidding. These are the type most commonly used in automotive applications (to support the wheels of a motor car for example), where they are used in pairs to accommodate axial thrust in either direction, as well as radial loads. They can support rather larger thrust loads than the ball type due to the larger contact area, but are more expensive to manufacture. Spherical roller thrust bearings use asymmetrical rollers of spherical shape, rolling inside a house washer with a raceway with spherical inner shape. They can accommodate combined radial and axial loads and also accommodate misalignment of the shafts. They are often used together with radial spherical roller bearings. Fluid bearings where the axial thrust is supported on a thin layer of pressurized liquid give low drag Magnetic bearings where the axial thrust is supported on a magnetic field They are used where very high speeds or very low drag are needed. Thrust bearings are commonly used in automotive, marine, and aerospace applications. They are also used in the main and tail rotor blade grips of RC (radio controlled) helicopters. Thrust bearings are used in cars because the forward gears in modern car gearboxes use helical gears which, while aiding in smoothness and noise reduction, cause axial forces that need to be dealt with. The double helical or herringbone gear balances the thrust caused by normal helical gears. One specific thrust bearing in an automobile is the clutch "throw out" bearing, sometimes called the clutch release bearing. Fluid-film thrust bearings were invented by Australian engineer George Michell who patented his invention in 1905. Michell bearings contain a number of sector-shaped pads, arranged in a circle around the shaft, and which are free to pivot. These create wedge-shaped regions of oil inside the bearing between the pads and a rotating disk, which support the applied thrust and

eliminate metal-on-metal contact. Michell's invention was notably applied to the thrust block in ships. The small size (one-tenth the size of old bearing designs), low friction and long life of Michell's invention made possible the development of more powerful engines and propellers. They were used extensively in ships built during World War I, and have become the standard bearing used on turbine shafts in ships and power plants worldwide.

1.5 Statement of the problem

The performance characteristics of a fixed incline slider bearing have not been investigated. The variation of pressure and temperature have not been studied. The friction coefficient and the power loss of a fixed incline slider bearing have also not be determined. The above mentioned is what this research attempts to address.

1.6 Broad objectives of the study

The general objective of the study was to analyze the variation of temperature, pressure and viscosity and geometry of the bearing on the performance of a fixed incline slider bearing.

1.7 Specific objectives of the study

The specific objectives of the study are;

1. To develop a mathematical model for a fixed inclined slider bearing
2. To determine the velocity profiles, pressure profiles and temperature profiles,
3. To determine the axial load (Normal load),

4. To determine friction coefficient and the power loss of a fixed incline slider bearing

1.8 Significance of the study

Rotating machinery is commonly used in our society for a wide range of energy conversions applications such as automobiles, electric power generation, cooling and ventilation. These are areas in mechanical engineering. Therefore, understanding the factors affecting the ability of a lube to lubricate surfaces in relative motion and how they correlate is important to the engineer. To improve the efficiency of a bearing, one may either alter the lubricant properties or alter the geometry of the bearing. Understanding the axial variation of pressure, temperature, viscosity, load and geometry of the bearing will be useful in the design of hydrodynamic bearings and in predicting the bearing performance.

CHAPTER TWO

LITERATURE REVIEW

2.1 Related Literature Review

A number of models of hydrodynamic bearings performance have been proposed over the years. Chang (2004) studied load capacity for adiabatic infinitely wide plane slider bearing in the turbulent thermo-hydrodynamic regime. They developed a two dimensional Navier-Stokes based model. Using Legendre collocation method, to analyse turbulent plane slider bearings with wide ranges of bearing configurations, mean Reynolds number and a parameter characterizing the viscosity variation. The load capacity formulation were established for turbulent isothermal and turbulent thermo-hydrodynamic bearings. With the equations provided in the study, the designers can quickly determine the load capacity without extensive.

Andrei and Traian (2005) analyzed theoretically the load carrying capacity of a typical thrust bearing with elastic pad in order to define optimal pad parameters using thrust bearing analysis software based on finite difference solution of flow and thermal equations and finite element solution for solid structure equations. The results represented for equivalent slider revealed that the load carrying capacity of such a bearing is comparable with a similar tilting-pad bearing. Zengeyu, Gadala and Segal(2006) studied a three dimensional modelling of thermo-hydrodynamic lubrication in slider bearings using streamline upwind petrovGalerkin method. The model couples the Reynolds and energy equations and was developed using the finite

element program. The model results indicate that the pick temperature is not on the mid-plane surface. This position shifting towards the mid-plane as the width to length ratio is reduced from 10 to 1 as well as when pressure boundary conditions are altered in such a way that the inlet/outlet pressure is higher than the side pressure. The adiabatic temperature profiles on infinite slider and square slider are compared. Model results show peak slide flow at a width-to-length ratio of 2.

Latif *et.al.* (2009)Studied thermo hydrodynamic performance of thrust bearings with circular tilted pads under the presence of air gas bubbles and centrifugal forces. He showed viscosity and density are altered substantially due to bubble presence as well as temperature rise and the influence of the centrifugal forces become significant as the speed become higher. They varied the geometry and loading parameters to show the combined effect on the bearing characteristic values. . Glavatskih (2009) wrote a paper on 3D thermo-hydrodynamic analysis of a textured slider with a temperature dependent fluid. Numerical solutions were carried out for a laminar and steady flow. Hot and cold lubricant mixing in the groove was modelled and examined for different operating conditions. The results obtained show that the texture has a stronger and positive influence on load carrying capacity when thermal effects are considered. This beneficial effect is a maximum for the longest dimples with a length shorter than the pad length. Texture is also beneficial for the load carrying capacity when the sliding speed and the inlet flow rate are varied. The load carrying capacity of the slider can be increased up to 16% in severe operating conditions (High sliding speed).

Kyung *et. al.* (2009) studied a three dimensional analysis of thermo-hydrodynamic performance of sector shaped, tilting pad thrust bearings. They studied the effect of pivot pistons and operating and environmental conditions on the bearing performance. They compared the analysis with iso-viscous or the two dimensional analysis and they

found it to predict the bearing performance. Maneshian (2009) studied thermo-hydrodynamic analysis of turbulent flow in journal bearings and presented their results based on the computational fluid dynamics techniques. In this analysis the numerical solution of the Navier-Stokes equation with the equation governing the kinetic energy of turbulence and the dissipation rate coupled with the energy equation in the lubricant flow and the heat conduction equation in the bearing are obtained. Considering the complexity of the physical geometry, conformal mapping is used to generate an orthogonal grid and the governing equations are transformed to computational domain. From these method, the lubricant velocity, pressure and temperature distributions in the circumferential and cross film directions are obtained without any approximation. The numerical results are compared with the experimental data and good agreement is found.

Chang *et. al* (2009) studied thermos-hydrodynamic lubrication analysis of misaligned plain journal bearing with surface roughness. They calculated the oil film pressure, oil film temperature, load carrying capacity and leakage flow rate, frictional coefficient and misalignment moment of a journal bearing with different angles of journal misalignment and surface roughness and considering oil VPR and thermal effect based on the generalized Reynolds equation, Energy equation and solid heat conduction equation. The result showed that the oil VPR and surface roughness have a significant effect on lubrication of misaligned journal bearings under large eccentricity ratio. Thus it is necessary to take the effect of journal misalignment, surface roughness, oil VPR and thermal effect into account in the design and analysis of journal bearings.

Boubendir *et. al.* (2011) did a research on the numerical study of the thermo-hydrodynamic lubrication phenomenon in porous journal bearings. In this study, a numerical simulation is presented for the thermo-hydrodynamic self-lubrication aspect analysis of porous circular journal bearing of finite length with seal ends. It consisted in analyzing the thermal effects on the behaviour of circular porous journal bearings. The Reynolds equation of this viscous films was used taking into account the oil leakage into the porous matrix by applying Darcy's law to determine the fluid flow in the porous media. The results showed that the temperature influence on journal bearings performance is important in some operating cases and that a progressive reduction in the pressure distribution in the load capacity and latitude angle is a consequence of the increasing permeability.

Marius (2012) researched on the influence of lubricant temperature on the functioning of hydrostatic guidance systems of machine tools. He made a functional simulation pattern of hydrostatic charging system which analyses the behavior of the lubricant under high temperature when it passes through a restrictor. Kiogora *et. al.* (2014) Developed a conservative scheme model of an inclined pad thrust bearing. They also obtained a numerical solution of the momentum and energy equations of an inclined pad thrust bearing. Banwait *et. al.* (2014) studied thermo-hydrodynamic analysis to investigate the influence of modified viscosity-temperature equation on a plain journal bearing. They used finite difference method to predict temperature distribution in a journal bearing. They found the temperature distribution along the axial direction of the journal using a steady state unidirectional heat conduction equation.

Charitupoulous *et. al.* (2014) did a computational investigation of thermo-hydrodynamic performance and mechanical deformations of fixed geometry thrust

bearing with artificial surface texting. Although a lot of research has been done in the last two decades, hydrodynamic analysis of an fixed incline slider bearing to determine its performance by considering axial variation of pressure, viscosity and temperature, load and the geometry of the bearing has not been researched on and this is what this research strived to explore.

CHAPTER THREE

METHODOLOGY

3.1 Assumptions and approximations

In the mathematical analysis, the lubricant to be used in a fixed incline slider bearing, the following assumptions were made;

i. Inertia and body force terms are negligible as compared to viscous and pressure forces
ii. The lubricant is incompressible
iii. There is no variation of pressure across the fluid film
iv. There is no slip in the fluid solid boundary
v. No external forces act on the film
vi. The fluid flow is assumed to be laminar

3.2 Governing Equations

Consider the flow of a Newtonian viscous incompressible fluid(lubricant) of constant density ρ and coefficient of viscosity η with velocity vector $\boldsymbol{q}$ having velocity components *u, v, w* and pressure p. The basic governing equations of fluid dynamics based on the assumptions above are;

3.2.1 Conservation of mass (Continuity Equation)

In three dimensions, the equation of continuity is;

$$\frac{\partial \rho}{\partial t} + \frac{\partial (\rho u)}{\partial x} + \frac{\partial (\rho v)}{\partial y} + \frac{\partial (\rho w)}{\partial z} = 0 \tag{3.1}$$

If the density is constant, i.e. $\frac{\partial \rho}{\partial t} = 0$, the equation becomes;

$$\frac{\partial u}{\partial x} + \frac{\partial v}{\partial y} + \frac{\partial w}{\partial z} = 0 \tag{3.2}$$

which is the equation of continuity for an incompressible fluid.

3.2.2 Conservation of momentum

This is derived from Newton's second law of motion which states that the sum of resultant forces is equal to rate of change of momentum of the flow. The momentum equation in is written as;

$$\frac{\partial \mathbf{q}}{\partial t} + (\mathbf{q}.\nabla)\mathbf{q} = -\frac{1}{\rho}\nabla p + \frac{1}{\rho}\nabla.\tau + \mathbf{F} \tag{3.3}$$

3.2.3 Reynolds Equation

The general Navier-Stokes equation in which inertia, body, pressure and viscous terms are included are sufficiently complicated to yield analytical solutions to most practical problems. There is however a class of flow condition known as "slow viscous motion" in which the pressure and viscous terms predominate. Fluid film lubrication problems fall into this category. The differential equations governing the pressure distribution of fluid film lubrication is known as the Reynolds equation. It was first derived by Osborne Reynolds (1886) . Reynolds restricted his analysis to

incompressible fluids. The Reynolds equation from the Navier- Stokes equation and the continuity equations can now be derived based on assumptions in 3.1.

Consider a fluid film of height h as shown below;

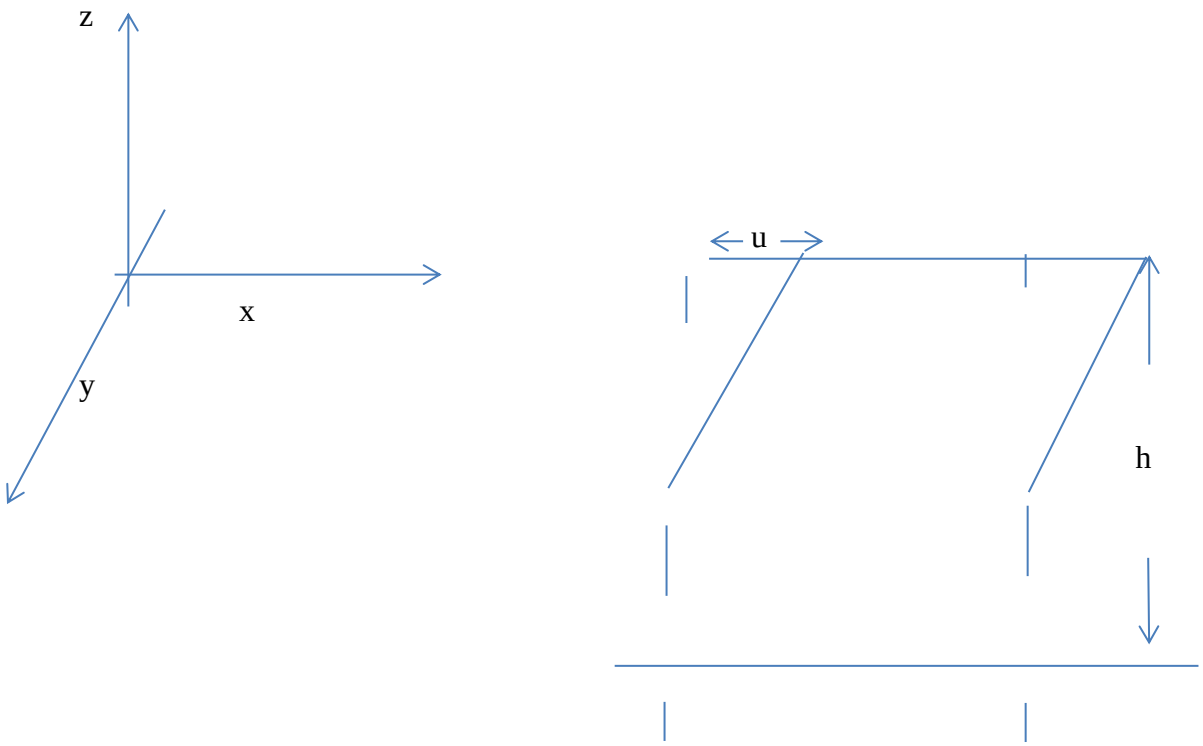

Figure: 3.1 Fluid depicting the shear (Source; Author, 2015)

Assuming that there is no variation of pressure across the fluid film, inertial and body force terms are negligible as compared to viscous and pressure forces, there is no slip in the fluid solid boundary and that the derivation of u and w with respect to y are much larger than derivation of velocity components, the Navier - Stokes equation (3.3) reduces to;

$$\frac{\partial p}{\partial x} = \frac{\partial}{\partial z}\left(\eta \frac{\partial u}{\partial z}\right)$$

$$\frac{\partial p}{\partial y} = \frac{\partial}{\partial z}\left(\eta \frac{\partial v}{\partial z}\right) \qquad (3.4)$$

Where η is the viscosity. Since p is a function of x and y only, the above equations can be integrated to obtain the generalized expressions for the velocity gradients;

$$\eta \frac{\partial u}{\partial z} = z \frac{\partial p}{\partial x} + A$$
$$\eta \frac{\partial v}{\partial z} = z \frac{\partial p}{\partial y} + C$$

Dividing through by η gives;

$$\frac{\partial u}{\partial z} = \frac{z}{\eta}\frac{\partial p}{\partial x} + \frac{A}{\eta}$$
$$\frac{\partial v}{\partial z} = \frac{z}{\eta}\frac{\partial p}{\partial y} + \frac{C}{\eta} \qquad (3.5)$$

Where A and C are integration constants. The viscosity of the lubricant may change considerably across the thin film (z direction) as a result of the temperature variations that arise in some bearing problem. For this case, we will treat η as the average value of viscosity across the film. This consideration will not restrict the variation of viscosity in the x and y directions. Therefore with η representing the average value of the viscosity across the film. Integrating the above equations gives;

$$u = \frac{z^2}{2\eta}\frac{\partial p}{\partial x} + A\frac{z}{\eta} + B$$

$$v = \frac{z^2}{2\eta}\frac{\partial p}{\partial y} + C\frac{z}{\eta} + D \qquad (3.6)$$

If zero slip at the fluid solid surface is assumed, the boundary values for velocity are;

1. z=0, u=u_b, v=v_b
2. z=h, u=u_a, v=v_a (3.7)

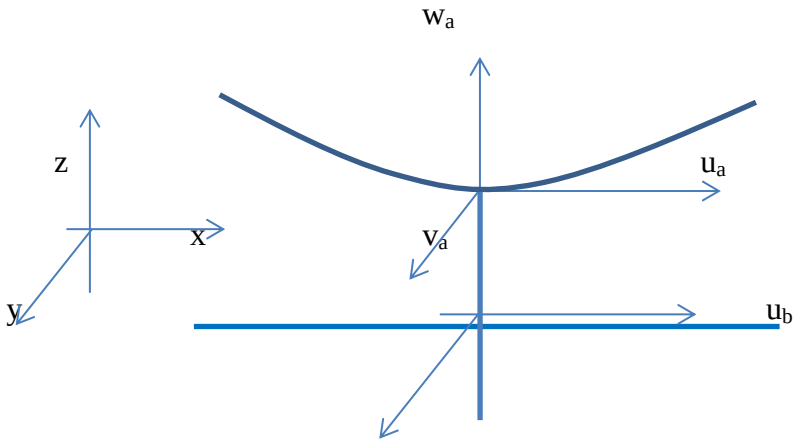

v_b w_b

Figure: 3.2 Fluid depicting velocity components(Source; Author, 2015)

The subscripts a and b refer to the conditions on the upper (curved) and lower (plane) surfaces respectively. Therefore u_a , v_a and w_a refer to the velocity components of the upper surface in the x,y and z directions respectively and u_b, v_b and w_b refer to the velocity components of the lower surface in the same directions. Applying the boundary conditions (3.7) to the equations above yields;

$$\frac{\partial u}{\partial z} = \left(\frac{2z-h}{2\eta}\right)\frac{\partial p}{\partial x} - \frac{u_a - u_b}{h} \tag{3.8a}$$

$$\frac{\partial v}{\partial z} = \left(\frac{2z-h}{2\eta}\right)\frac{\partial p}{\partial y} - \frac{v_a - v_b}{h} \tag{3.8b}$$

$$u = -z\left(\frac{h-z}{2\eta}\right)\frac{\partial p}{\partial x} + u_b\frac{h-z}{h} + u_a\frac{z}{h} \tag{3.9b}$$

$$v = -z\left(\frac{h-z}{2\eta}\right)\frac{\partial p}{\partial y} + v_b\frac{h-z}{h} + v_a\frac{z}{h} \tag{3.9b}$$

The viscous shear stresses acting on a solid can be expressed as;

$$\tau_{zx} = \eta\left(\frac{\partial w}{\partial x} + \frac{\partial u}{\partial z}\right) \tag{3.10a}$$

$$\tau_{zy} = \eta\left(\frac{\partial w}{\partial y} + \frac{\partial v}{\partial z}\right) \tag{3.10b}$$

In the order of magnitude evaluation, $\frac{\partial w}{\partial z}$ and $\frac{\partial w}{\partial y}$ are much smaller than $\frac{\partial u}{\partial z}$ and $\frac{\partial v}{\partial z}$

, therefore;

$$\tau_{zx} = \eta\frac{\partial u}{\partial z}$$

$$\tau_{zy} = \eta\frac{\partial v}{\partial z} \tag{3.11}$$

and the viscous shear stress acting on the upper and lower solid surfaces can be expressed while making use of equations 3.8 as;

$$\left(\tau_{zx}\right)_{z=0} = \left(\eta \frac{\partial u}{\partial x}\right)_{z=0} = \frac{-h}{2}\frac{\partial p}{\partial x} - \frac{\eta\left(u_b - u_a\right)}{h} \tag{3.12a}$$

$$\left(-\tau_{zx}\right)_{z=h} = -\left(\eta \frac{\partial u}{\partial z}\right)_{z=h} = \frac{-h}{2}\frac{\partial p}{\partial x} + \frac{\eta\left(u_b - u_a\right)}{h} \tag{3.12b}$$

$$\left(\tau_{zy}\right)_{z=0} = \left(\eta \frac{\partial v}{\partial z}\right)_{z=0} = \frac{-h}{2}\frac{\partial p}{\partial y} - \frac{\eta\left(v_b - v_a\right)}{h} \tag{3.12c}$$

$$\left(-\tau_{zy}\right)_{z=h} = -\left(\eta \frac{\partial v}{\partial z}\right)_{z=h} = \frac{-h}{2}\frac{\partial p}{\partial y} + \frac{\eta\left(v_b - v_a\right)}{h} \tag{3.12d}$$

The volume flow rate per unit width in the x and y directions are defined as;

$$q_x^{'} = \int_0^h u dz$$

(3.13a)

$$q_y^{'} = \int_0^h v dz \tag{3.13b}$$

Substituting equations 3.9 in these equations gives;

$$q_x^{'} = \frac{-h^3}{12\eta}\frac{\partial p}{\partial x} + \frac{u_a + u_b}{2}h$$

(3.14a)

$$q_y^{'} = \frac{-h^3}{12\eta}\frac{\partial p}{\partial y} + \frac{v_a + v_b}{2}h \tag{3.14b}$$

Returning to equations 3.9 the Reynolds equation is formed by introduction these expressions into the continuity equation 3.1

Let as first express the continuity equation in integral form;

$$\int_0^h \left(\frac{\partial \rho}{\partial t} + \frac{\partial}{\partial x}\left(\rho u\right) + \frac{\partial}{\partial y}\left(\rho v\right) + \frac{\partial}{\partial z}\left(\rho w\right)\right) dz = 0 \tag{3.15}$$

Now from integration rules;

$$\int_0^h \frac{\partial}{\partial x}[f(x,y,z)]dz = -f(x,y,z)\frac{\partial h}{\partial x} + \frac{\partial}{\partial x}\left(\int_0^h f(x,y,z)dz\right) \tag{3.16}$$

If ρ is the mean density, across the film, the u component term in the integrated equation is;

$$\int_0^h \frac{\partial}{\partial x}(\rho u)dz = -(\rho u)_{z=h}\frac{\partial h}{\partial x} + \frac{\partial}{\partial x}\left(\int_0^h \rho u dz\right) = -\rho u_a \frac{\partial h}{\partial x} + \frac{\partial}{\partial x}\left(\rho\int_0^h u dz\right) \tag{3.17}$$

Similarly for the v component;

$$\int_0^h \frac{\partial}{\partial y}(\rho v)dz = -\rho v_a \frac{\partial h}{\partial y} + \frac{\partial}{\partial y}\left(\rho\int_0^h v dz\right) \tag{3.18}$$

The w component term can be integrated directly to give;

$$\int_0^h \frac{\partial}{\partial z}(\rho w)dz = \rho(w_a - w_b) \tag{3.19}$$

Therefore the integrated continuity equation becomes;

$$h\frac{\partial \rho}{\partial t} - \rho u_a \frac{\partial h}{\partial x} + \frac{\partial}{\partial x}\left(\rho\int_0^h u dz\right) - \rho v_a \frac{\partial h}{\partial y} + \frac{\partial}{\partial y}\left(\rho\int_0^h v dz\right) + \rho(w_a - w_b) = 0 \tag{3.20}$$

The integrals in this equation represents the volume flow rates per unit width $q_x^{'}$ and $q_y^{'}$ described in equations 3.14 above. Introducing the flow rates expressions into the continuity equation yields the general Reynolds equation;

$$-\frac{\partial}{\partial x}\left(\frac{\rho h^3}{12\eta}\frac{\partial p}{\partial x}\right) + \frac{\partial}{\partial y}\left(\frac{-\rho h^3}{12\eta}\frac{\partial p}{\partial y}\right) + \frac{\partial}{\partial x}\left(\frac{\rho h(u_a + u_b)}{2}\right) + \frac{\partial}{\partial y}\left(\rho h\frac{(v_a + v_b)}{2}\right) + \rho(w_a - w_b) - \rho u_a \frac{\partial h}{\partial x} - \rho v_a \frac{\partial h}{\partial y} + h\frac{\partial \rho}{\partial t} = 0 \tag{3.21}$$

3.2.4 Reduced form of Reynolds equation

If the fluid motion is purely tangential, where $w_a = u_a \frac{\partial h}{\partial x} + v_a \frac{\partial h}{\partial y}$ and $w_b = 0$, the general Reynolds equation (3.21) becomes;

$$\frac{\partial}{\partial x}\left(\frac{\rho h^3}{\eta}\frac{\partial p}{\partial x}\right) + \frac{\partial}{\partial y}\left(\frac{\rho h^3}{\eta}\frac{\partial p}{\partial y}\right) = 12\mu\frac{\partial(\rho h)}{\partial x} + 12\upsilon\frac{\partial(\rho h)}{\partial y} \tag{3.22}$$

Where;

$$u = \frac{u_a + u_b}{2} = \text{constant} \text{ and } v = \frac{v_a + v_b}{2} = \text{constant}$$

For hydrodynamic lubrication, the fluid property do not vary significantly throughout the bearing and this may be considered to be constant. Also, for hydrodynamic lubrication, the motion is purely sliding so that the velocity is zero. Thus the corresponding Reynolds equation is;

$$\frac{\partial}{\partial x}\left(h^3\frac{\partial p}{\partial x}\right) + \frac{\partial}{\partial y}\left(h^3\frac{\partial p}{\partial y}\right) = 12u\eta\ \frac{\partial h}{\partial x} \tag{3.23}$$

Equation 3.22 above does not only allow the fluid properties to vary in the x and y directions, but also permits the bearing surface to be of finite length in the y direction. Side leakage or flow in the y direction is associated with the second and third equations in 3.22 and 3.23

Neglecting side leakages;

$$\frac{\partial}{\partial x}\left(\frac{\rho h^3}{\eta}\frac{\partial p}{\partial x}\right) = 12u\frac{\partial(\rho h)}{\partial x} \tag{3.24}$$

This equation can be integrated with respect to x to give;

$$\frac{1}{\eta}\frac{dp}{dx} = \frac{12u}{h^2} + \frac{A}{\rho h^3} \tag{3.25a}$$

Making use of the boundary conditions;

$\frac{dp}{dx} = 0$ when $x = x_m, \rho = \rho_m, h = h_m$ gives;

A= $-12\, u\rho_m h_m$

Substituting this into equation 3.25a gives;

$$\frac{dp}{dx} = 12u\eta \frac{\rho h - \rho_m h_m}{\rho h^3} \tag{3.25b}$$

This is the integrated form of the Reynolds equation. The subscript refers to the condition at all points where $\frac{dp}{dx} = 0$, such as the point of maximum pressure. If the density does not vary much throughout the conjunction, it can be considered to be constant so that;

$$\frac{dp}{dx} = 12u\eta \frac{h - h_m}{h^3} \tag{3.26}$$

3.3 Dimensional analysis

Dimensional analysis is very useful for planning, presentation and interpretation of experimental data. Most practical fluid mechanic problems are too complex to solve analytically and must be tested by experiment or approximated by computational fluid dynamics. These data have much more generality if they are expressed in compact economical non-dimensional form. Dimensional analysis is a method for reducing the number of complexity of experimental variables that affect a given physical phenomena.The non-dimensional numbers numbers in hydrodynamics applicable to this study can now be defined;

3.3.1 Reynolds number

This is denoted by Re and is defined as the ratio of inertia forces ρU_0^2 to viscous forces $\frac{\mu U_o}{L_o}$.

$$\mathrm{Re} = \frac{\rho U_0 L_0}{\mu} = \frac{U_0 L_0}{\upsilon}$$

3.3.2 Prandtl Number

$$P_r = \frac{\mu c_p}{\kappa}$$

In heat transfer involving convection warm and cool particles mix and because of their temperature difference, local heat conduction occurs. This mixing also involves momentum transfers. Prandtl's Number is a measure of the relative ability of the fluid to allow momentum diffusion and thermal diffusion.

3.3.3 Stribeck number

The stribeck number is defined as $S_t = \frac{\mu_0 u_0}{P_0}$ and is used to categorize the friction properties between two surfaces. These categories are; boundary lubrication mixed lubrication and hydrodynamic lubrication. In this research, the Stribeck number will be chosen for hydrodynamic lubrication. In addition, the ratio $\frac{r_0}{H_0}$ is chosen to be equal to 10^{-3}. This is the standard quantity for a typical thrust bearing pad.

3.3.4 Pressure coefficient

This is also referred to as the Euler's number. It is defined as $P_c = \frac{p_0}{\rho U_0^{\,2}}$. It gives the importance of pressure term relative to inertia term.

3.4 Force components and oil film geometry

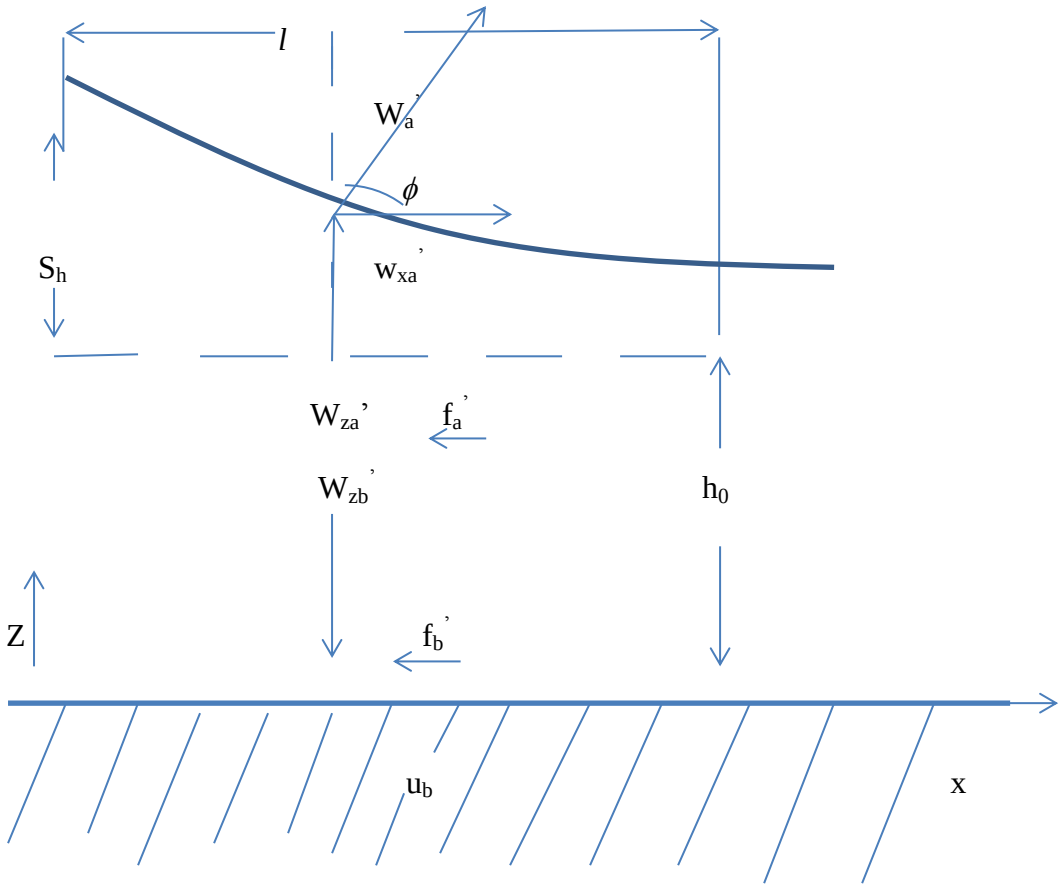

Figure 3.1: Force components and oil film geometry in a hydrodynamically lubricated thrust sector. (Source; Author, 2015)

The forces acting on the solids can be considered in two groups. The loads, which act in the direction normal to the surface, yield normal loads that can be resolved into components w_x' and w_z'. The viscous surface stresses, which act in the direction tangent to the surface, yield shear forces on the solids that have components f' in the x direction. The component of the shear forces in the z direction is negligible. Once the

pressure is obtained for a particular film configuration from the Reynolds equation, the following force components act on the solids:

$$w'_{za} = w'_{zb} = \int_0^l p\,dx \tag{4.1}$$

$$w'_{xb} = 0 \tag{4.2}$$

$$w'_{xa} = -\int_{h_0+sh}^{h_0} p\,dh = -\int_0^l p\frac{dh}{dx}dx$$

$$\therefore w'_{xa} = -(ph)_0^l + \int_0^l h\frac{dp}{dx}dx = \int_0^l h\frac{dp}{dx}dx \tag{4.3}$$

$$w'_b = \left(w'^{\,2}_{zb} + w'^{\,2}_{xb}\right)^{\frac{1}{2}} = w'_{zb} \tag{4.4}$$

$$w'_a = \left(w'^{\,2}_{za} + w'^{\,2}_{xa}\right)^{\frac{1}{2}} \tag{4.5}$$

$$\phi = \tan^{-1}\frac{w'_{xa}}{w'_{za}} \tag{4.6}$$

Shear forces per unit width acting on the solids are;

$$f'_b = \int_0^l (\tau_{zx})_{z=0}\,dx$$

From equation (3.12),

$$(\tau_{zx})_{z=0} = \left(\eta\frac{\partial u}{\partial z}\right)_{z=0} = \frac{-h}{2}\frac{\partial p}{\partial x} - \eta\frac{(u_b - u_a)}{h}$$

Therefore substituting this in the equation above gives;

$$f'_b = \int_0^l \left(\frac{-h}{2}\frac{dp}{dx} - \eta\frac{u_b}{h}\right)dx$$

Making use of equation (4.3) yields;

$$f'_b = -\frac{w'_{xa}}{2} - \int_0^l \frac{\eta u_b}{h}dx \tag{4.7}$$

Similarly the shear force per unit width acting on the solid a is;

$$f_a^{'} = -\int_0^l (\tau_{zx})_{z=h}\, dx = \frac{-w_{xa}^{'}}{2} + \int_0^l \frac{\eta u_b}{h} dx \tag{4.8}$$

Note from figure 4.1.1 that;

$$f_b^{'} + f_a^{'} - w_{xa}^{'} = 0 \tag{4.9}$$

$$w_{zb}^{'} - w_{za}^{'} = 0 \tag{4.10}$$

These equations represent the condition of static equilibrium. The viscous stresses generated by the shearing of the lubricant film give rise to a resisting force of magnitude $-f_b$ on the moving surface. The rate of working against the viscous stresses, or power loss is

$$h_p = -f_b u_b = -f_b^{'}(r_0 - r_i)u_b \tag{4.11}$$

The work done against the viscous stresses appears as heat within the lubricant. Some of this heat may be transferred to the surroundings by radiation or by conduction, or it may be convected from the clearance space by the lubricant flow. The bulk temperature rise of the lubricant for the case in which all the heat is carried away by convection is known as the "adiabatic temperature rise." This bulk temperature increase can be calculated by equating the rate of heat generated within the lubricant to the rate of heat transferred by convection:

$$h_p = \rho q C_p (\Delta t_m)$$

Or the adiabatic temperature rise in degrees Celsius may be expressed as;

$$\Delta t_m = \frac{hp}{\rho q C_p} \tag{4.12}$$

Where ρ=density of the lubricant, kg/m^3

q=Volume flow rate in the direction of motion, m^3/s

C_p=Specific heat of material at constant pressure, J/kg^{0}C

The equations above can now be used to analyze a fixed inclined slider bearing. In the analysis, we will make use of non-dimensiolization to define the resulting performance parameters of the bearing. It will be assumed that the pressure generating mechanism is the physical wedge.

4.2 Fixed incline slider bearing

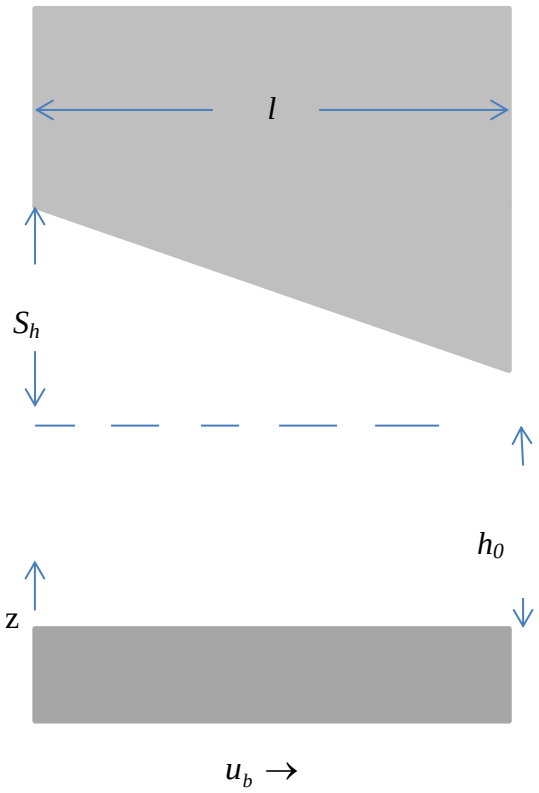

Figure 4.2: Fixed incline slider bearing (Source; Author, 2015)

The figure 3.21 above shows a fixed incline slider bearing. A fixed incline slider bearing consists of two non-parallel plane surfaces separated by an oil film. One surface is stationary while the other moves with a uniform velocity. The direction of motion and the inclination of planes are such that a converging oil film is formed

between the surfaces and the physical wedge pressure-generating mechanism is developed in the oil film; it is this pressure-generating mechanism that makes the bearing able to support a load.

4.2.1 Pressure distribution

For hydro dynamic lubrication, the Reynolds equation is given by;

$$\frac{\partial}{\partial x}\left(h^3\frac{\partial p}{\partial x}\right)+\frac{\partial}{\partial y}\left(h^3\frac{\partial p}{\partial y}\right)=12u\eta\frac{\partial h}{\partial x} \tag{4.13}$$

Neglecting side leakages, equation (4.13) becomes;

$$\frac{\partial}{\partial x}\left(\frac{\rho h^3}{h}\frac{\partial p}{\partial x}\right)=12u\eta\frac{\partial(\rho h)}{\partial x} \tag{4.14}$$

Integrating this equation with respect to x gives;

$$\frac{1}{\eta}\frac{dp}{dx}=\frac{12u}{h^2}+\frac{A}{\rho h^3} \tag{4.15}$$

Making use of the boundary conditions that;

$\frac{dp}{dx}=0$ when $x=x_m$ $\rho=\rho_m$ $h=h_m$ gives;

$A=-12u\rho_m h_m$

Substituting this into equation (4.15) gives;

$$\frac{dp}{dx}=12u\eta\frac{\rho h-\rho_m h_m}{\rho h^3} \tag{4.16}$$

This is the integrated form of the Reynolds equation. The subscript m refers to the condition at all points where $\frac{dp}{dx}=0$ such as the point of maximum pressure.

If the density does not vary much throughout the conjunction, then it can be considered constant and equation 4.16 reduces to;

$$\frac{dp}{dx} = 12u\eta \frac{h - h_m}{h^3} \tag{4.17}$$

We will begin the analysis of an inclined slider bearing with the integrated form of Reynolds equation (4.17) above. Keeping in mind that $u = \frac{u_a + u_b}{2}$ If we let $u_a=0$, and assuming a constant viscosity η_0, Equation (4.17) becomes;

$$\frac{dp}{dx} = 6\eta_0 u_b \frac{h - h_m}{h^3} \tag{4.18}$$

Where h_m is the film thickness when $\frac{dp}{dx} = 0$ The oil film thickness can be written as a function of x;

$$h = h_0 + s_h\left(1 - \frac{x}{l}\right) \tag{4.19}$$

Expressing the film thickness and pressure in dimensionless terms yields;

$$P = \frac{ps_h^{\,2}}{\eta_0 u_b l}, \text{H}=\frac{h}{s_h}, \; H_m = \frac{h_m}{s_h}, \; H_0 = \frac{h_0}{s_h} \text{ and } X = \frac{x}{l} \tag{4.20}$$

Incorporating this in equation (4.18) and (4.19) gives,

$$\frac{dP}{dx} = 6\left(\frac{H - H_m}{H^3}\right) \tag{4.21}$$

$$H = \frac{h}{s_h} = H_0 + 1 - X \tag{4.22}$$

$$\frac{dH}{dX} = -1 \tag{4.23}$$

Integrating equation (4.21) gives;

$$P = 6\int\left(\frac{1}{H^2} - \frac{H_m}{H^3}\right)dX$$

Making use of equation (4.23) , gives;

$$P = -6\int\left(\frac{1}{H^2} - \frac{H_m}{H^3}\right)dH$$

$$P = 6\left(\frac{1}{H} - \frac{H_m}{2H^2}\right) + A \qquad (4.24)$$

The boundary conditions are;

1. P=0 when X=0→ H=H_0+1
2. P=0 when X=1→H=H_0

Making use of boundary conditions 1 and 2 we get;

$$H_m = \frac{2H_0(1+H_0)}{1+2H_0} \qquad (4.25)$$

and $A = -\frac{6}{1+2H_0}$ (4.26)

Substituting equations (4.25) and (4.26) into (4.24) gives;

$$P = \frac{6X(1-X)}{(H_0+1-X)^2(1+2H_0)} \qquad (4.27)$$

Next, we determine the maximum pressure for the incline slider bearing, as we saw earlier, the pressure is maximum, (i.e. $\frac{dp}{dx} = 0$), $X = X_m, H = H_m,$ Therefore substituting this in (4.22), gives;

$$H_m = H_0 + 1 - X_m$$

Rearranging;

$$X_m = \frac{1+H_0}{1+2H_0} \qquad (4.28)$$

Substituting this in equation (4.27), yields;

$$P_m = \frac{3}{2H_0(1+H_0)(1+2H_0)} \qquad (4.29)$$

In dimensionless terms, equation (4.29) becomes

$$p_m = \frac{3\eta_0 u_b l s_h}{2h_0(s_h + h_0)(s_h + 2h_0)} \tag{4.30}$$

4.2.2 Normal load component

The normal load per unit width can be written as;

$$w_z' = \int_0^l p dx$$

The equation can be written in dimensionless form by making use of relations (4.20)

$$W_z = \frac{w_z' s_h^2}{\eta_0 u_b l^2} = \int_0^1 P dX$$

Because $\frac{dH}{dX} = -1$,

$$W_z = -\int_{H_0+1}^{H_0} P dH \tag{4.31}$$

Substituting equations (4.24) to (4.26) into this (4.31) gives;

$$W_z = 6\ln\left(\frac{H_0 + 1}{H_0}\right) - \frac{12}{1 + 2H_0} \tag{4.32}$$

These results are based on the knowledge of the assumptions that side leakage was neglected and smooth surfaces and isothermal conditions were assumed.

4.2.3 Tangential Force Components

The force per unit width in the direction of motion due to pressure being developed is;

$$w'_{xb} = 0$$

$$w'_{xa} = -\int_{h_0+s_h}^{h_0} pdh$$

Making use of equation (4.20), the preceding equation may be expressed in dimensional form as

$$W_{xa} = \frac{w'_{xa}}{\eta_0 u_b}\frac{s_h}{l} = -\int_{H_0+1}^{H_0} PdH = W_z \tag{4.33}$$

4.2.4 Shear Force Components

The shear force components per unit width acting on the solids are;

$$f'_b = \int_0^l (\tau_{zx})_{z=0}\, dx = \int_0^l \left(\eta_0 \frac{\partial u}{\partial z}\right)_{z=0} dx$$

$$f'_a = \int_0^l (-\tau_{zx})_{z=h}\, dx = -\int_0^l \left(\eta_0 \frac{\partial u}{\partial z}\right)_{z=h} dx \tag{4.34}$$

The viscous shear stresses are defined as;

$$(\tau_{zx})_{z=0} = \left(\eta \frac{\partial u}{\partial z}\right)_{z=0} = \frac{-h}{2}\frac{\partial p}{\partial x} - \frac{\eta(u_b - u_a)}{h} \tag{4.35}$$

$$(-\tau_{zx})_{z=h} = \left(\eta \frac{\partial u}{\partial z}\right)_{z=h} = \frac{-h}{2}\frac{\partial p}{\partial x} - \frac{\eta(u_b - u_a)}{h}$$

Substituting equations (4.35) into (4.34) while letting u_a=0 we have;

$$f'_b = -\int_0^l \left(\frac{h}{2}\frac{dp}{dx} + \frac{u_b \eta_0}{h}\right) dx$$

$$f'_a = -\int_0^l \left(\frac{h}{2}\frac{dp}{dx} - \frac{u_b \eta_0}{h}\right) dx \tag{4.36}$$

Expressing (4.15) in dimensionless form using equations (4.20) yields;

$$F_b = \frac{f_b^{'}}{\eta_0 u_b}\frac{s_h}{l} = -\int_0^1 \left(\frac{H}{2}\frac{dP}{dX} + \frac{1}{H}\right)dX$$

$$F_a = \frac{f_b^{'}}{\eta_0 u_b}\frac{s_h}{l} = -\int_0^1 \left(\frac{H}{2}\frac{dP}{dX} - \frac{1}{H}\right)dX \qquad (4.37)$$

By making use of equations (4.20), the preceding equations can be expressed as;

$$F_b = 4\ln\left(\frac{H_0}{H_0+1}\right) + \frac{6}{1+2H_0}$$

$$F_a = 2\ln\left(\frac{H_0}{H_0+1}\right) + \frac{6}{1+2H_0} \qquad (4.38)$$

4.2.5 Friction coefficient

The friction coefficient can be expressed as;

$$\mu = \frac{-f_b^{'}}{w_{zb}^{'}} = \frac{f_a^{'} + w_{xa}^{'}}{w_{za}^{'}}$$

Making use of equations (4.21) and (4.22) gives;

$$\mu = \frac{2s_h \ln\left(\frac{H_0}{H_0+1}\right) + \frac{3s_h}{1+2H_0}}{3l\ln\left(\frac{H_0}{H_0+1}\right) + \frac{6l}{1+2H_0}} \qquad (4.39)$$

4.2.6 Volume flow rate

The volume flow rate per unit width can be expressed as,

$$q_x^{'} = -\frac{h^3}{12\eta}\frac{\partial p}{\partial x} + \frac{h(u_b + u_a)}{2} \qquad (4.40)$$

Evaluating the flow rate where $\frac{dp}{dx} = 0$ and setting u_a=0 gives the volume rate as;

$$q_x = \frac{u_b h_m}{2} \tag{4.41}$$

The dimensionless volume flow rate can be expressed as;

$$Q = \frac{2q_x^{'}}{u_b s_h} = H_m = \frac{2H_0(1+H_0)}{1+2H_0} \tag{4.42}$$

4.2.7 Power Loss and Temperature Rise

The total rate of working against the viscous stresses, or the power loss, can be expressed from (4.11) as,

$$h_p = -f_b u_b = -f_b^{'}(r_0 - r_i)u_b$$

Expressed in dimensionless form,

$$H_p = \frac{h_p s_h}{\eta_0 u_b{}^2 l(r_0 - r_i)} = \frac{-f_b^{'} s_h}{\eta_0 u_b l} = F_b$$
$$= -4\ln\left(\frac{H_0}{H_0+1}\right) - \frac{6}{1+2H_0} \tag{4.43}$$

All the heat produced by viscous shearing is assumed to be carried away by the lubricant(adiabatic condition) The bulk temperature increase can be calculated by equating the rate of heat generated within the lubricant to the rate of heat transferred by convection. Therefore from equation (4.12), the lubricant temperature rise is;

$$\Delta t_m = \frac{h_p}{\rho_0 q_x^{'} C_p} = \frac{2u_b l \eta_0 H_p}{\rho_0 C_p s_h{}^2 Q} \tag{4.44}$$

Where;

ρ_0 = The constant lubricant density, Kg/m^3

$q_x^{'}$ = The volume flow rate per unit width in sliding direction, m^2/s

C_p=specific heat of constant pressure J/kgC

The dimensionless temperature rise may be expressed as;

$$\frac{\rho_0 C_p s_h{}^2 \Delta t_m}{2u_b l \eta_0} = \frac{H_p}{Q} = \frac{2(1+2H_0)}{H_0(1+H_0)} \ln\left(\frac{H_0+1}{H_0}\right) - \frac{3}{(1+H_0)H_0} \tag{4.45}$$

4.2.8 Centre of Pressure

The location of the center of pressure x_{cp} indicates the position at which the resulting force is acting. The expression for calculating the location is given by;

$$w_z' x_{cp} = \int_0^l pxdx = \frac{\eta_0 u_b l^3}{s_h{}^2} \int_0^1 PXdX$$

Therefore the dimensionless center of pressure can be written as

$$X_{cp} = \frac{x_{cp}}{l} = \frac{1}{w_z} \int_0^1 PXdX \tag{4.46}$$

Substituting equation (4.22) to (4.24) into (4.46) gives;

$$X_{cp} = -\frac{6}{w_z(1+2H_0)} \left[(H_0+1)(3H_0+1) \ln\left(\frac{H_0}{H_0+1}\right) + 3H_0 + \frac{5}{2} \right] \tag{4.47}$$

4.2.9 Velocity Profile and Stream Function

For a stationary top surface, (u_a=0), the fluid velocity can be written as;

$$u = \frac{-z(h-z)}{2\eta_0} \frac{dp}{dx} + \frac{u_b(h-z)}{h} \tag{4.48}$$

Using equations (4.22), this equation can be expressed in the dimensionless form as;

$$\frac{u}{u_b} = \left(1 - \frac{Z}{H}\right)\left(1 - \frac{ZH}{2}\frac{dP}{dX}\right) \tag{4.49}$$

Where $Z = \frac{z}{s_h}$ and 0≤Z≤H

(4.50)

From equation (4.49), $\frac{u}{u_b} = 0$ when;

1. $Z_{cr} = H$ or at the top surface

2. $Z_{cr} = \frac{2}{H\left(\frac{dP}{dX}\right)}$ (4.51)

Note that condition 2 can only exist when $\frac{dP}{dX} > 0$ and thus when $X<X_m$

Substituting equation (4.21) into equation (4.51) while making sure that the inequality in equation (4.50) is satisfied gives;

$0 \leq 2H - 3H_m$ (4.52)

Making use of equations (4.22) and (4.25) gives

$$X \leq \frac{1 - H_0^2}{2H_0 + 1} \tag{4.53}$$

The inequality is only satisfied if $H_0 \leq 1$. This then implies that reverse flow exists when;

$H_0 \leq 1$ and $X \leq \frac{1 - H_0^2}{2H_0 + 1}$ (4.54)

If these inequality is satisfied, then;

$\frac{dP}{dX} > 0$ and $X < X_m$

Substituting equation (4.21) into equation (4.49) gives;

$$\frac{u}{u_b} = \left(1 - \frac{Z}{H}\right)\left[1 - \frac{3Z}{H}\left(1 - \frac{H_m}{H}\right)\right] \tag{4.55}$$

Where $\frac{Z}{H} = \frac{Z}{H_0 + 1 - X}$

$$\frac{H_m}{H} = \frac{2H_0(1 + H_0)}{(1 + 2H_0)(H_0 + 1 - X)} \tag{4.56}$$

Thus, $\frac{u}{u_b}$ is just a function of X, Z and H_0.A streamline is a curve tangent to which gives the fluid velocity vector. Surface boundaries are streamlines since the fluid cannot cross the surface boundary. The definition of streamline may be given mathematically while neglecting the side leakage term as;

$$\frac{dx}{u} = \frac{dz}{w} \tag{4.57}$$

The continuity equation for an incompressible fluid is given by;

$$\frac{\partial u}{\partial x} + \frac{\partial v}{\partial y} + \frac{\partial w}{\partial z} = 0$$

This equation can be satisfied while neglecting the side leakage term by introducing a new function defined by;

$$u = \frac{\partial \phi}{\partial z} \text{ and } w = -\frac{\partial \phi}{\partial x} \tag{4.58}$$

Where ϕ is a function of x and z and is called the stream function. By using the chain rule of partial differentiation, the total derivative of ϕ can be expressed as;

$$d\phi = \frac{\partial \phi}{\partial x} dx + \frac{\partial \phi}{\partial z} dz \tag{4.59}$$

Making use of equation (4.58), gives;

$$d\phi = -w dx + u dz \tag{4.60}$$

Setting dϕ=0, the definition of a streamline given in equation (4.57) is obtained. Equation (4.58) can also be expressed in dimensionless terms of a stream function ϕ as ;

$$\frac{u}{u_b} = \frac{1}{u_b}\frac{\partial \phi}{\partial z} = \frac{\partial \Phi}{\partial Z} \tag{4.61}$$

Where $\Phi = \dfrac{\phi}{u_b s_h}$

Substituting equation (4.55) into equation and integrating gives;

$$\Phi(x,z) = \frac{Z^3}{6}\frac{dP}{dX} - \frac{Z^2}{2H}\left(1 + \frac{H^2}{2}\frac{dP}{dX}\right) + Z = \text{constant} \tag{4.62}$$

Also from the continuity equation and neglecting the side leakage term, the velocity in the Z direction can be written as;

$$w = \int\left(-\frac{\partial u}{\partial x}\right)dz = \frac{s_h u_b}{l}\int\left(\frac{\partial\left(u/u_b\right)}{\partial X}\right)dZ$$

$$\therefore \frac{w}{u_b}\frac{l}{s_h} = -\int_0^Z\left[\frac{\partial\left(u/u_b\right)}{\partial H}\right]\frac{\partial H}{\partial X}dZ = \int_0^Z\left(\frac{\partial\left(u/u_b\right)}{\partial H}\right)dZ$$

Substituting equation (4.55) into this equation gives

$$\begin{aligned}\frac{wl}{u_b s_h} &= \left(Z^2 - \frac{Z^3}{H}\right)\left(\frac{2}{H^2} - \frac{3H_m}{H^3}\right) \\ &= \frac{Z^2}{H^4}(Z-H)(3H_m - 2H)\end{aligned} \tag{4.63}$$

Note from this equation that

$\frac{w}{u_b}\left(\frac{l}{s_h}\right)=0$ when Z=0. When Z=H, and at $H=\frac{3}{2}H_m$. Making use of equation (4.22) and (4.25) gives the critical value of X where $H=\frac{3}{2}H_m$ as;

$$X_{cr}=\frac{1-H_0^2}{1+2H_0}$$

(4.64)

Note that $0\leq X_{cr}\leq 1$ when $H_0\leq 1$

CHAPTER FOUR

RESULTS AND DISCUSSION

From equation (4.27) dimensionless pressure, P is a function of X and H_0.

Table 4.1: The variation of P with X for various values of H_0

X	0	0.2	0.4	0.6	0.8	1.0
H_0=2, P	0	0.0244	0.0426	0.05	0.0396	0
H_0=1, P	0	0.0987	0.1875	0.244	0.222	0
$H_0=\frac{1}{2}$,P	0	0.2840	0.5950	0.888	0.979	0
$H_0=\frac{1}{4}$,P	0	0.580	1.328	2.272	3.160	0

From equation 4.32,

$$W_z = 6\ln\left(\frac{H_0+1}{H_0}\right) - \frac{12}{1+2H_0}$$

Table 4.2: The table of values for W_z and H_0

Dimensionless Normal load carrying capacity, W_z	∞	0.591	0.129	0.064	0.032
Film thickness ratio, H_0	0	0.5	1	1.5	2

Table 4.3: The table of values for dimensionless force components W_{xa}, F_b and F_a

Film thicknesss ratio H_0	0.2	0.4	0.6	0.8	1.0	1.2
$W_{xa=}W_z$	2.179	0.849	0.430	0.250	0.158	0.107
F_b	-2.881	-1.677	-1.196	-0.936	-0.772	-0.659
F_a	0.702	0.827	0.765	0.685	0.613	0.552

From equation (4.39), the friction coefficient is given as;

$$\mu = \frac{2s_h \ln\left(\frac{H_0}{H_0+1}\right) + \frac{3s_h}{1+2H_0}}{3l \ln\left(\frac{H_0}{H_0+1}\right) + \frac{6l}{1+2H_0}} \qquad (5.2)$$

Clearly, the friction coefficient is a function of s_h, l and H_0. Setting s_h=1 and l=3, gives

$$\mu = \frac{2\ln\left(\frac{H_0}{H_0+1}\right) + \frac{3}{1+2H_0}}{9\ln\left(\frac{H_0}{H_0+1}\right) + \frac{18}{1+2H_0}}$$

Table 4.4: The table of values for friction coefficient μ versus film thickness H_0

Film thickness ratio H_0	0	0.5	1	1.5	2
Friction coefficient μ	∞	0.785	1.620	2.788	4.288

The dimensionless volume flow rate Q is given by equation 4.42 as;

$$Q = \frac{2H_0(1+H_0)}{1+2H_0} \qquad (5.3)$$

Table 4.5: A table of values for Q versus H_0 is shown below;

Film thickness ratio, H_0	0	0.5	1	1.5	2.0
Dimensionless volume flow rate, Q	0	0.75	1.333	1.875	2.40

From equation (4.45), the dimensionless adiabatic temperature rise is given by;

$$\frac{\rho_0 C_p s_h{}^2 \Delta t_m}{2u_b l \eta_0} = \frac{H_p}{Q} = \frac{2(1+2H_0)}{H_0(1+H_0)} \ln\left(\frac{H_0+1}{H_0}\right) - \frac{3}{(1+H_0)H_0} \qquad (5.4)$$

Table 4.6: The table of values for adiabatic temperature rise versus film thickness

Film thickness ratio H_0	0	0.5	1.0	1.5	2.0
Adiabatic temperature rise $\frac{H_p}{Q}$	∞	1.859	0.579	0.289	0.175

The dimensionless Power Loss (Rate of working against viscous forces) is given by 4.43 as;

$$H_p = -4\ln\left(\frac{H_0}{H_0+1}\right) - \frac{6}{1+2H_0} \qquad (5.5)$$

Table 4.7: A table of values for Dimensionless power loss versus film thickness ratio

Film thickness ratio, H_0	0	0.5	1	1.5	2
Dimensionless power loss, H_p	∞	1.3944491547	0.7725887222	0.5433024951	0.4218604324

The graph of P versus X for various values of H_0 is as shown below;

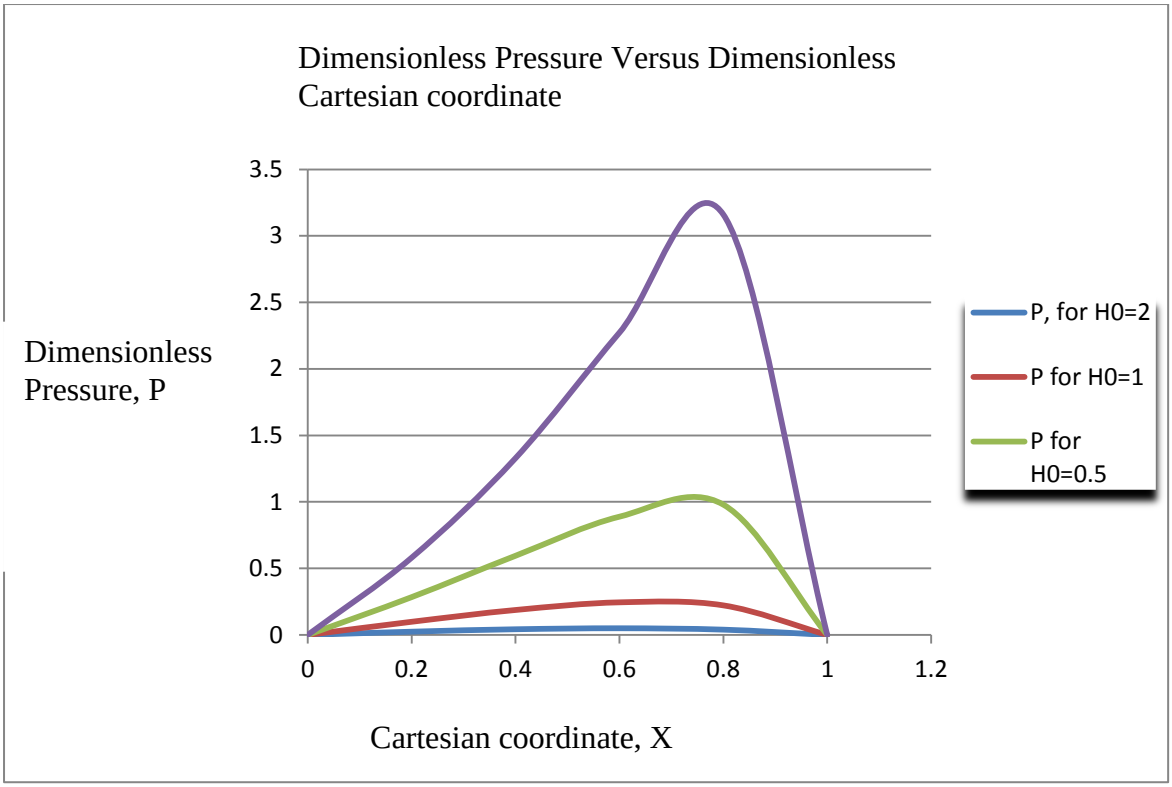

Figure 5.1: Graph of dimensionless Pressure, P versus dimensionless Cartesian coordinate X

From figure 5.1, it is clear that Pressure distribution increases with decreasing H_0.

Since $H_0 = \frac{h_0}{s_h}$, if the shoulder height s_h is kept constant, the graph above indicates that as the outlet film thickness h_0 becomes smaller, the pressure profile increases without any limits. The figure also shows that for large H_0, there is little pressure build up for a fixed incline slider bearing. From equation (4.28), As $H_0 \rightarrow 0$, the location of the maximum pressure $X_m \rightarrow 1$. But as $H_0 \rightarrow \infty$, $X_m \rightarrow \frac{1}{2}$. Further, $H_0 \rightarrow 0$ implies that either $h_0 \rightarrow 0$ or $s_h \rightarrow \infty$. But $H_0 \rightarrow \infty$, implies that either $h_0 \rightarrow \infty$ or $s_h \rightarrow 0$. The situation of $s_h \rightarrow 0$, implies parallel surfaces, and parallel surfaces do not develop pressure. From equation (4.30), it is observed that $s_h \rightarrow 0$, which corresponds to a parallel film, and $s_h \rightarrow \infty$ both produce $p_m \rightarrow 0$. The shoulder height that produces maximum pressure can be obtained from

$\frac{\partial p_m}{\partial s_h} = 0.$ Evaluating this gives;

$$(s_h)_{opt} = \sqrt{2}h_0 \qquad (5.1)$$

Equation (5.1) will be useful in the design of fixed incline slider bearings. For instance, if the shoulder height s_h is known ,one can predict what the minimum outlet film thickness h_0 should be. The shoulder height can then be established by using the safety factor.

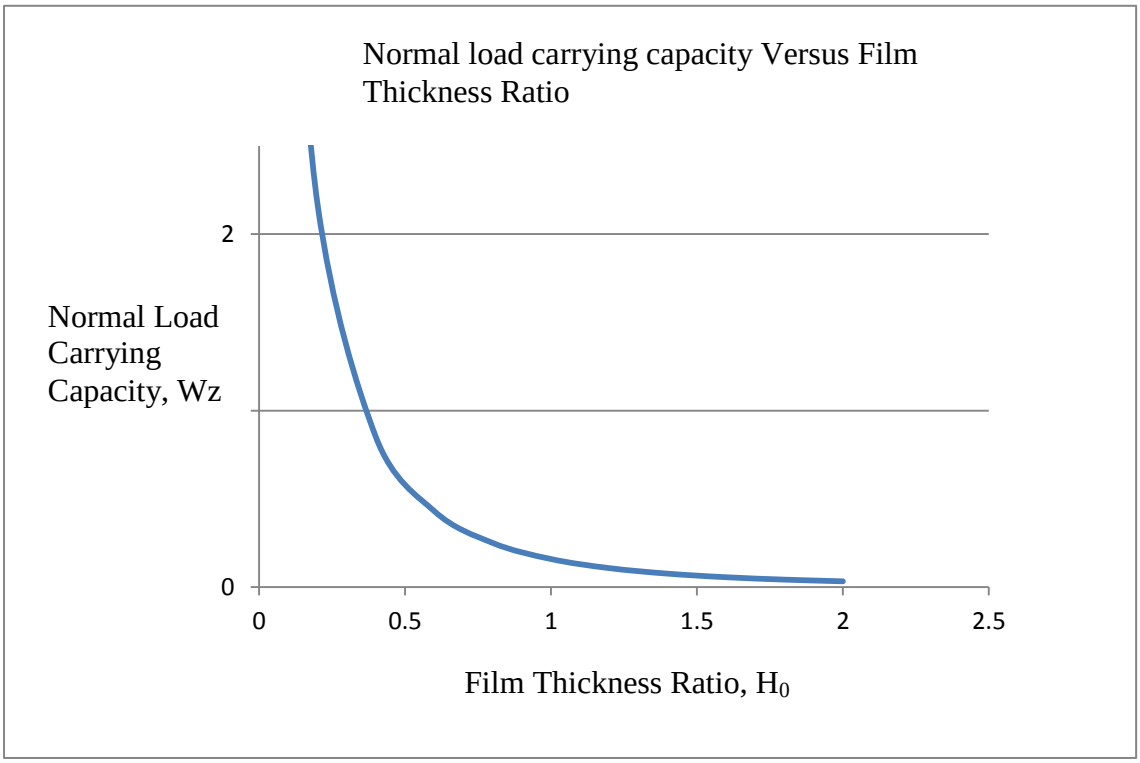

Figure 5.2: Variation of film thickness ratio with normal load carrying capacity

Figure 5.2 shows that as $H_0 \rightarrow 0$, the potential of this bearing to support a load increases exponentially.

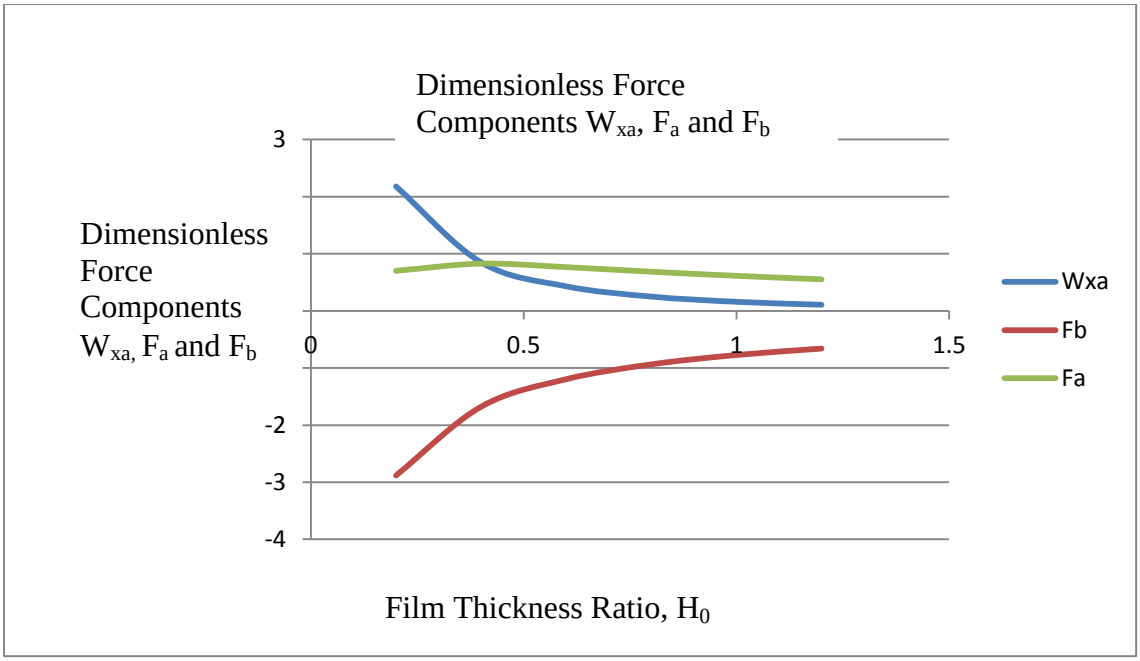

Figure 5.3 Effect of film thickness ratio on force components

The dimensionless force components W_{xa}, F_b and F_a are plotted as functions of H_0 in figure 5.3 above. The graph of friction coefficient μ versus film thickness H_0 is as shown below;

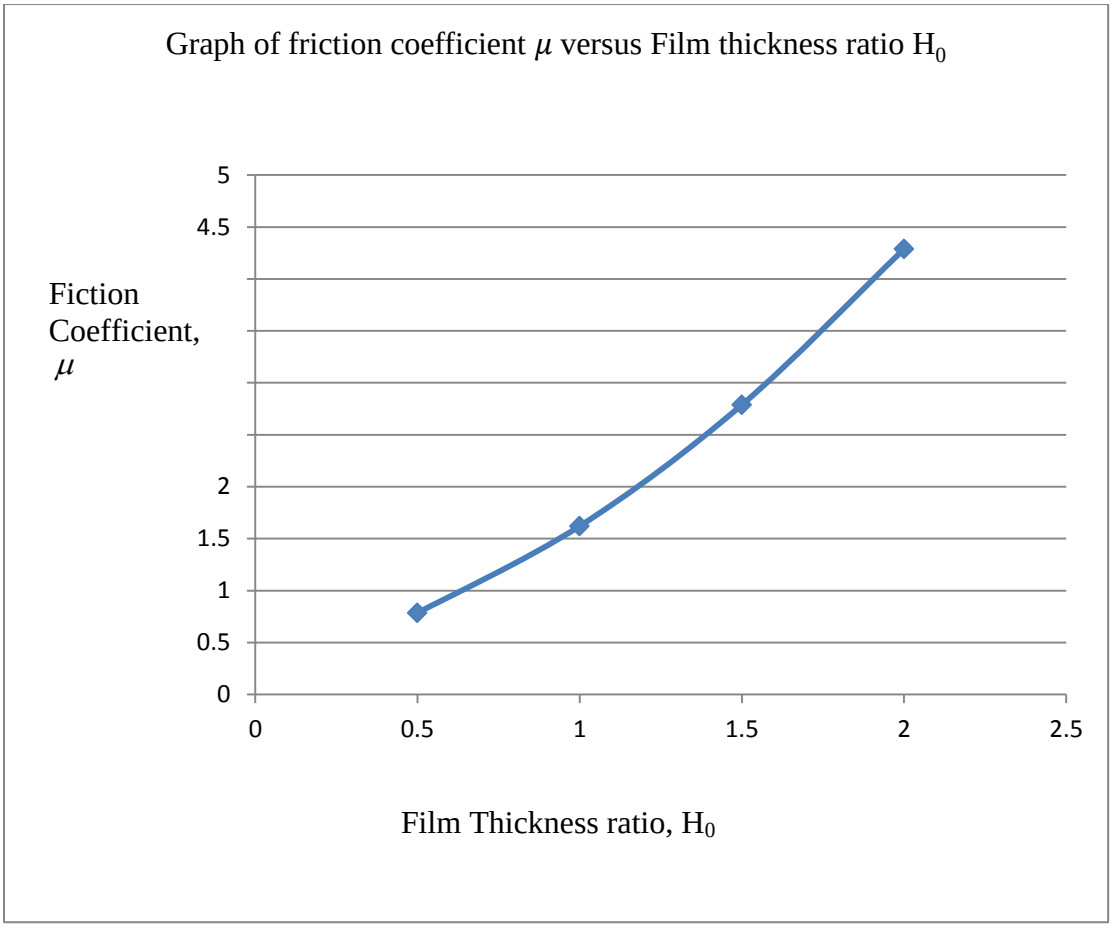

Figure 5.4: Effect of film thickness ratio on friction coefficient

From the graph, the frictional force parameter μ increases exponentially with increasing H_0

A graph of Q versus H_0 is shown below;

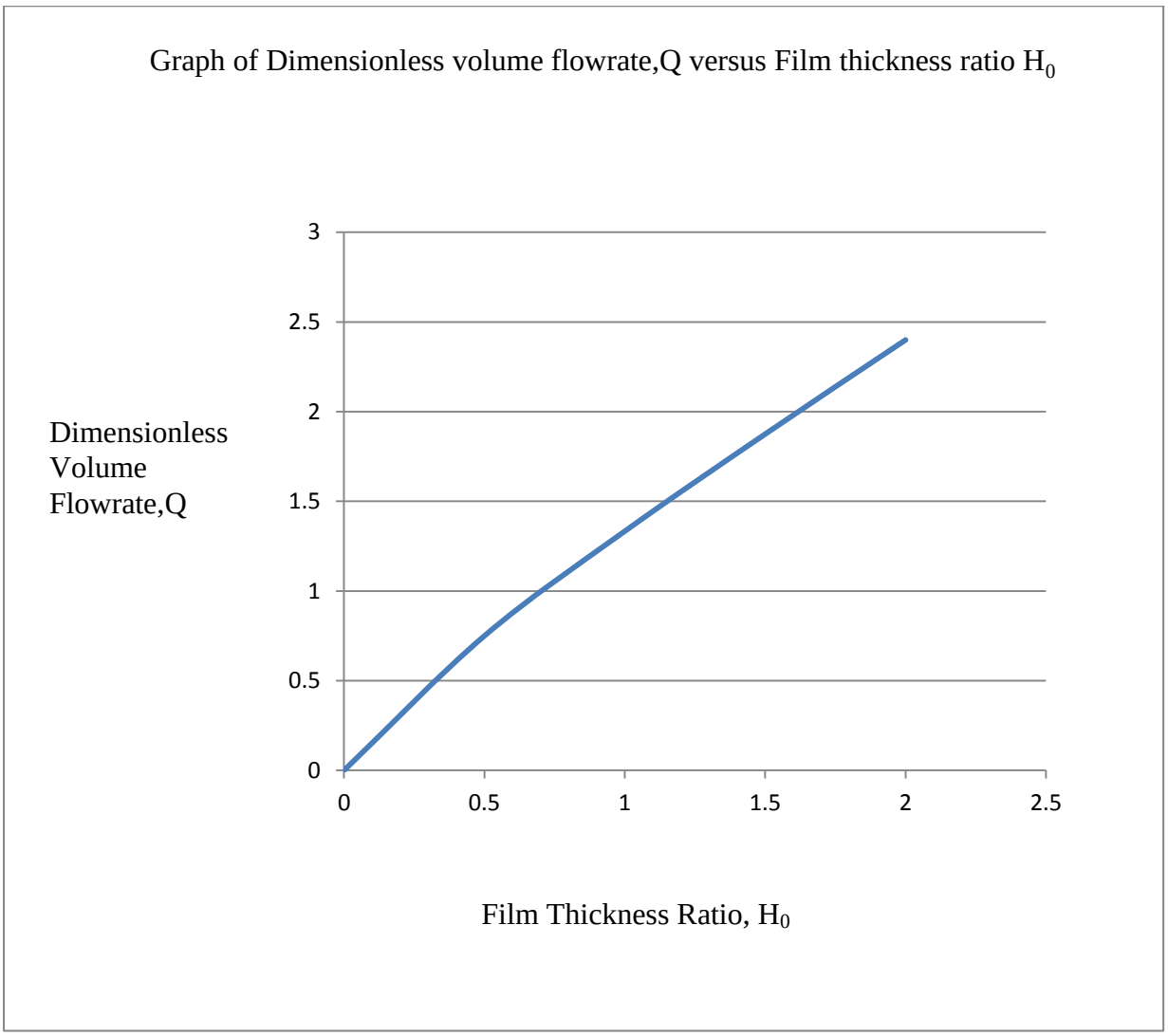

Figure 5.5: Effect of film thickness ratio on volume flow rate

The graph of adiabatic temperature rise versus film thickness ratio is as shown below;

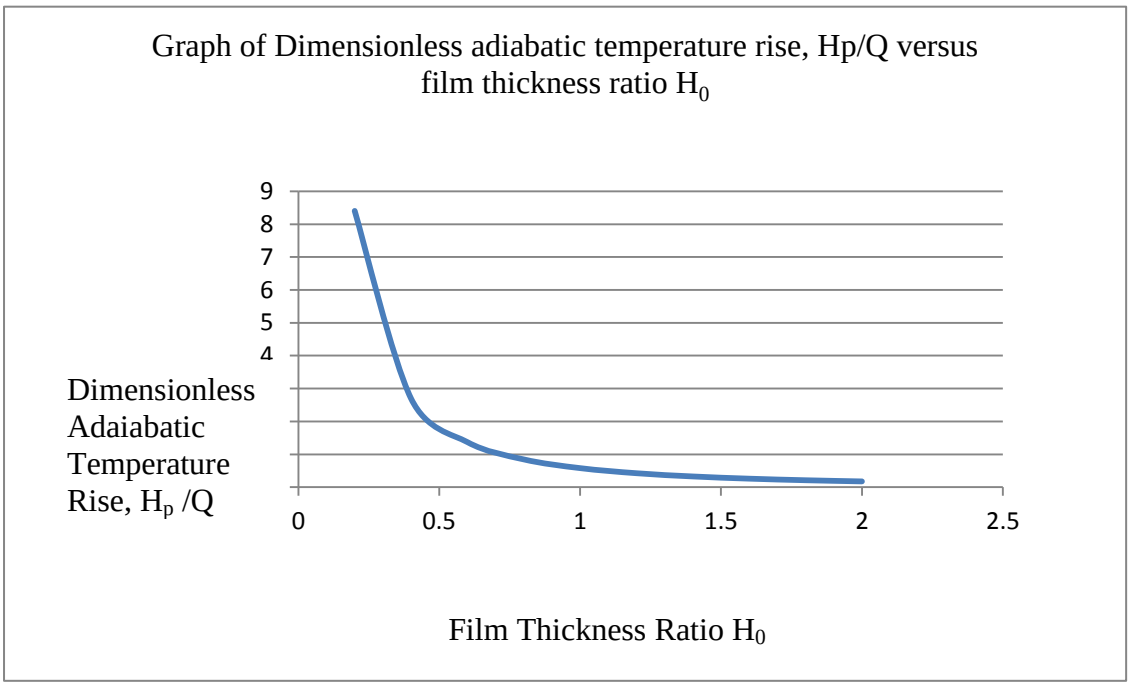

Figure 5.6: Effect of film thickness ratio on adiabatic temperature rise

A graph of Dimensionless power loss versus film thickness ratio is shown below;

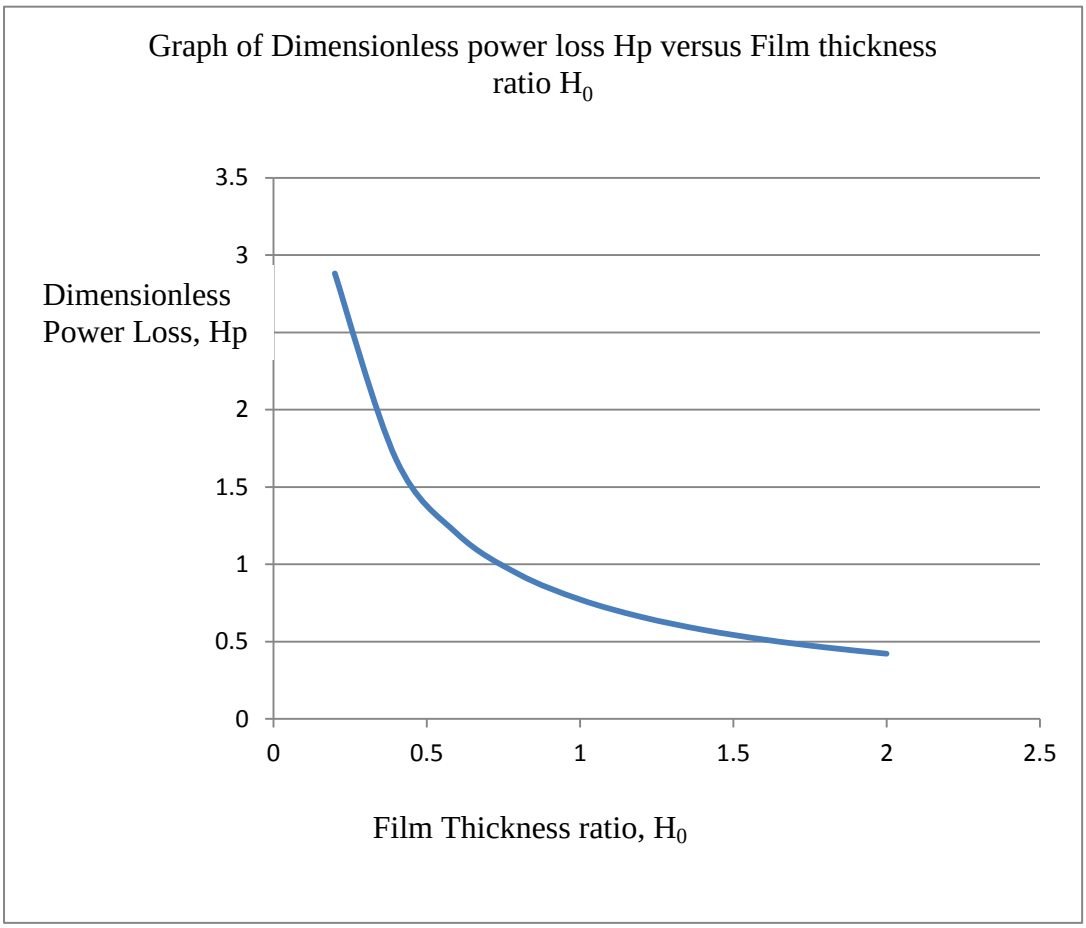

Figure 5.7: Effect of film thickness ratio on power loss

CHAPTER FIVE

CONCLUSION AND RECOMMENDATION

5.1 Conclusion

In this research, the analysis of the axial variation of various parameters on the flow of the lubricants under hydrodynamic lubrication condition between the plates of a fixed incline slider bearing has been done. The equations governing hydrodynamic flow considered in our study namely; the continuity equation, the Navier-stokes equations, the Reynolds equation. The Navier-stokes equation together with the continuity equation is used to derive the Reynolds equation. The Reynolds equation is then used to determine the pressure distribution of the lubricant in a fixed incline slider bearing. The normal load components, friction coefficient, volume flow rates, tangential and shear force components, power loss and temperature rise are determined and their variation along the bearing analyzed, discussed and represented graphically. In particular:

1. The pressure profiles are in good agreement with published results for the bearing done in two dimensions
2. The pressure profiles are in good agreement with published results for studies of thermos-hydrodynamic lubrication of a tilting pad step bearing.

This proves the fidelity of our model.

5.2 Recommendation

The author recommends the following;

1. Due to variation in the pressure build up and thermal effects , a full fluid film condition may not always be attained. Therefore there is need to extend the study to a elasto-hydrodynamic and boundary lubrication analysis.
2. In the research, the fluid flow was considered to be laminar. The same research can be carried out by considering a turbulent case.
3. Also, in the research, a fixed incline slider bearing was considered. One may wish to carry out the same research on other types of bearings namely; Journal bearing, Step bearing etc.
4. The research was carried out by keeping the viscosity of the lubricant constant. One can carry out the same research by considering the variations of lubricants viscosity.

REFFERENCES

Shiuh-Hwa Shyu, Yeau-Ren Jeng and Chi-Cheng Chang(2004): "Load capacity for adiabatic infinitely wide wide plane slider bearings in the turbulent thermohydrodynamic regime" *Journal of Tribology*, vol. 47 pp (396-401).

Miles Zengeyu, Mohamed Gadala and Guus segal(2006): " Three dimensional modelling of thermo-hydrodynamic lubrication in slider bearings" *International journal of computation and methodology* vol. 49, issue 10, pp 947-968

B. Maneshian and S.A. GandJalikh Nassab (2009) "Thermohydrodynamic analysis of turbulent flow in journal bearings running under different steady conditions" *IJE Transactions* vol. 223, issue number 8, pp. 1115-1127

L.A. Abdel Latif, E.M. Bakr and M.I. Ghobrial (2009): "Centrifugal effects of thermo hydrodynamic performance of circular pad thrust bearings" *Journal of tribology* issue no.111(3) pp 510-517

Kyung Woong Kim (2009) "A three dimensional analysis of thermohydrodynamic performance of sector-shaped tilting –pad thrust bearings." *ASME Journal of tribology technology*, Issue no. 105, pp. 406-412

Sergei Glavatskih, Samuel Cupillard and Michel Cervantes (2009) "3D Thermo-hydrodynamic analysis of a textured slider with a temperature dependant fluid". *Tribology international*, Issues no. 10, pp. 1487-1495.

Jun Sun, Mei Deng and Yong Hong Fu and Chang Lin Gui(2009) "Thermo-hydrodynamic analysis of misaligned plain journal bearing with surface roughness" *Journal of tribology* 132(1). pp. 1115

S. Bounbendir, S. Larbi and R. Bennacer(2011): ”Numerical study of the thermo-hydrodynamic lubrication phenomenon in porous Journal bearings” *Tribology international*, vol 44, issue no. 1, pp 1-8

Pascu Marius(2012): “ the influence of lubricants temperature on the functions of hydrostatic guidance systems*.” Journal of Engineering studies and research* Vol 18. Issue No. 4 pp. 71-77

Charitopoulos A., Fouflias D., Papadopoulos C.I., Kaiktsis L., Fill on M. (2013): “Computational Investigation of Thermo-elasto-hydrodynamic (TEHD) Lubrication in a Textured Sector-Pad Thrust Bearing” *Journal of tribology*, vol. 15, pp. 403-411

P.R. Kiogora, M.N. Kinyanjui, David M Theuri. (2014):“Conservative scheme model of an inclined thrust pad thrust bearing*”. International Journal of Engineering Science and innovative technology*, Vol. 3 Issue 1, pp 446-453

P.R. Kiogora, M.N. Kinyanjui, David M Theuri (2014): ”Numerical solution of the momentum and energy equations of an inclined pad thrust bearing”. *International Journal of Engineering Science and innovative technology*, Vol. 3, issue 3, pp 381-388

K.r. Kadam and S.S. Banwait (2014): “ The influence of modified viscosity-temperature equation on thermo-hydrodynamic analysis of plain journal bearing” *American journal of mechanical engineering* Vol 2 Issue no. 6, pp. 169-177.